ROLE OF SUDDEN COMMENCEMENTS IN TRIGGERING MAGNETOSPHERIC SUBSTORMS

by

RICHARD ERIN NEWELL

A thesis submitted in partial fulfillment

of the requirements for the degree of

MASTER OF SCIENCE

UNIVERSITY OF WASHINGTON

Approved by George K. Parks
(Chairman of Supervisory Committee)

Department Geophysics Program
(Departmental Faculty Sponsoring Candidate)

Date May 16, 1974

Master's Thesis

In presenting this thesis in partial fulfillment of the requirements for a master's degree at the University of Washington, I agree that the Library shall make its copies freely available for inspection. I further agree that extensive copying of this thesis is allowable only for scholarly purposes. It is understood, however, that any copying or publication of this thesis for commercial purposes, or for financial gain shall not be allowed without my written permission.

Signature Richard E. Nowell

Date 5/16/74

TABLE OF CONTENTS

LIST OF FIGURES

LIST OF TABLES

ACKNOWLEDGEMENTS

The author wishes to thank the NOAA Commissioned Corps and the NOAA Space Environment Laboratory, Boulder, Colorado, for providing this opportunity for schooling and research. Special thanks go to Dr. George K. Parks of the Space Sciences Division of the University of Washington's Geophysics Program, whose guidance and encouragement helped to see this work through. Appreciation is also extended to the other members of the Supervisory Committee, Drs. Stewart W. Smith, Kenneth C. Clark, and Ward J. Helms. Thanks are due to Dr. James I. Vette of World Data Center A, Greenbelt, Maryland, for providing the Explorer data, to Mr. Donald J. Hei, Jr., of that organization for helpful talks regarding data availability and reliability, to Dr. J. R. Winckler of the University of Minnesota for providing ATS 1 electron flux data, and to Drs. P. J. Coleman and R. L. McPherron of the University of California, Los Angeles, for providing ATS 1 magnetic field data.

This research was supported in part by the Atmospheric Sciences Section of the National Science Foundation under grants 33021x, GA-33719, and GU-2655, and by the National Aeronautics and Space Administration under grant NGR 48-002-154.

INTRODUCTION

A fundamental problem in connection with magnetospheric substorms is the identification of triggering mechanisms. In this regard, it is of considerable importance to understand why certain sudden commencements (sc's) trigger substorms while others do not. Heppner [1955] was the first to note that sc's often occur near the time of auroral-zone magnetic bay onsets, and Haurwitz [1969] concluded that such bay onsets are activated by sc-associated phenomena. Schieldge and Siscoe [1970] showed that conditions favoring simultaneous sc-associated magnetospheric compressions and magnetic bay onsets include a depressed low-latitude geomagnetic field H component in the pre-midnight sector, as well as relatively high compressional amplitudes. The latter condition was independently verified by Kawasaki et al. [1971]. Finally, Burch [1972] concluded that the necessary and sufficient conditions for the triggering of simultaneous polar magnetic bay onsets by sc's are (1) an sc amplitude of more than 10γ and (2) an average southward interplanetary magnetic field component of less than -1γ over a period of at least one-half hour preceding the sc.

The above studies deal with the relationship between sc-associated interplanetary conditions and accompanying polar magnetic bay onsets. As yet, no systematic investigation has been made of the magnetospheric conditions at and near the time of sc events. Such information is needed in order to determine if certain magnetospheric conditions are necessary for the occurrence of the bay onsets. Accordingly, this study examines sc events in terms of available auroral-zone and low-latitude magnetic field data, interplanetary plasma and magnetic field data, and magnetospheric electron flux

and magnetic field data from the geostationary satellite ATS 1.

PRESENTATION OF DATA

The data used in this study include observations obtained at the earth's surface, in the magnetosphere, and in interplanetary space. Most of these observations apply to the times at and near thirty-seven sudden commencement events occurring within the period January 1967 through July 1968 (see Figure 1). Examples of this data are presented in Figures 2 through 7. Availability of the sc-associated data, by date and data type, is described in Table 1.

General Description

The ground-based observations consist of (a) magnetograms from polar, auroral, and low-latitude stations, and (b) time profiles of the A_E index, a geomagnetic activity index derived from the data of selected auroral-zone magnetometer stations. This index represents the envelope of the horizontal component of the magnetogram traces from the given stations, and is intended to portray the Universal-Time variations of the ionospheric auroral electrojet activity (see Figure 6). Individual magnetograms were used to supplement the A_E data when the need for more detailed information arose. The high-latitude magnetometer stations are listed in Table 2 and their locations are plotted in Figures 8 and 9. The low-latitude stations are located at Honolulu (21.3°N, 158.0°W), San Juan (18.1°N, 66.2°W), and Tashkent (41.3°N, 69.6°E). The average magnitude of the sc-related enhancement of the horizontal magnetic field component at these three stations was used to

represent the magnitude of the sc, following Kawasaki et al. [1971] and Burch [1972]. The sudden commencements studied here were well-documented events, each observed by at least ten magnetometer stations from the global network. The timing of the events was determined by averaging the near-simultaneous sc times reported by the observing stations. These times signal the impingement on the magnetosphere of a discontinuity in the solar wind, usually observed as an abrupt increase of geomagnetic field strength. The times are published in "Solar-Geophysical Data", a monthly publication of the Department of Commerce, available from the National Climatic Center, Asheville, North Carolina. The A_E data and individual magnetograms were provided by World Data Center A for Solar-Terrestrial Physics, Boulder, Colorado.

The magnetospheric data, observed at the synchronous, equatorial orbit of the ATS 1 satellite, include (a) magnetometer data (D, H, and V components, centered at and rotating with the earth, where H is in the direction of the earth's spin vector, V is positive radially outward from the earth, and D is positive eastward, completing the right-handed system) and (b) electron flux data (50-150 keV, 150-500 keV, 500 keV - 1 MeV). These data were helpful in inferring changes in magnetospheric compression, configuration, and particle content. Time profiles of the data were made available directly by the organizations conducting the data-collection experiments, namely UCLA (magnetometer) and the University of Minnesota (electron spectrometer). Data were also provided on microfilm by the National Space Science Data Center (NSSDC) in Greenbelt, Maryland.

The interplanetary data used in this study were (a) magnetometer data

(magnetic field magnitude, horizontal angle, and vertical angle) from Explorers 33 and 35, and (b) plasma data (particle density, bulk speed, and thermal speed) from Explorers 33, 34, and 35. The magnetic field was observed primarily in the Geocentric Solar Equatorial (GSEq) coordinate system. This interplanetary data helped us to evaluate the behavior of the solar wind and its frozen-in magnetic field at and near the time of the sudden commencement events. The data were furnished by NSSDC in the form of printed and microfilmed tables and microfilmed time profiles. Fine-time-scale plasma data from Explorers 33 and 35 were also made available in the form of computer print-outs by Mr. Don Hei of NSSDC. Plots of solar ecliptic plane projections of the trajectories of the three satellites, produced by Behannon et al. [1970], were supplied on microfiche by NSSDC.

Specific Parameters

The parameters used in this study were chosen on the basis of (1) data availability and (2) apparent relevance to the problems being studied here. The definitions and general significance of these parameters are as follows:

$\overline{\delta H_{SFC}}$: the average enhancement of the horizontal components of the magnetic field at Honolulu, San Juan, and Tashkent, occurring simultaneous with the sc, i.e., within ± 5 minutes of t_{sc}. This is taken to indicate the magnitude of the geomagnetic field compression associated with the sudden commencement.

δH_{ATS}: any pronounced sc-simultaneous (±5 minutes) enhancement of the horizontal component of the magnetic field at ATS 1. This, like $\overline{\delta H_{SFC}}$, should indicate the magnitude of the magnetic field compression associated

with the sudden commencement.

ΔH_{ATS}: this is equal to H - $\overline{H_{QQ}}$, where H is taken at t_{sc}, just before the δH_{ATS} enhancement. $\overline{H_{QQ}}$ is the average value of H at that same time of day for the four quietest days of that month, similar to the original definition of Cummings et al. [1969]. Negative ΔH_{ATS} corresponds to a depression of H below quiet-time values. Such a depression is commonly interpreted to indicate a tail-like nightside magnetic field [Coleman and Cummings, 1971], characterized by enhanced dawn-dusk plasma sheet current together with an earthward-convecting (magnetospherically-inflating) plasma sheet [Russell, 1972].

$\overline{B}$: magnitude of the interplanetary magnetic field (IMF), averaged over the half-hour period preceding t_{sc}.

$\overline{\theta}$: average IMF vertical (latitudinal) angle in Geocentric Solar Equatorial coordinates, where the x-axis is along the earth-sun line, positive sunward, the z-axis is parallel to the sun's rotational axis, positive northward, and the y-axis completes the right-handed Cartesian coordinate system.

$\overline{\phi}$: average IMF horizontal (azimuthal) angle in GSEq coordinates.

$\overline{B_z}$: average IMF z-component in GSEq coordinates, equal to $\overline{B}\sin\overline{\theta}$. Negative values of B_z have been shown to be related to many aspects of geomagnetic activity, including H_{ATS} depression [Aubrey and McPherron, 1971] and polar magnetic bay development [Fairfield and Cahill, 1966; Rostoker and Falthammer, 1967; Wilcox et al., 1967; Schatten and Wilcox, 1967; Fairfield, 1968; Hirshberg and Colburn, 1969; Arnoldy, 1971]. The half-hour averaging period used for these IMF parameters was found to be relatively effective in

organizing the data, in agreement with Burch [1972].

δB, $\delta\phi$, $\delta\theta$, δB_z: the magnitude of an abrupt change of the corresponding IMF component occurring within ±5 minutes of t_{sc}. Large, abrupt changes in B_z have been observed to be associated with significant changes in geomagnetic activity [Meng et al., 1973].

$\overline{N}$, δN: solar wind plasma density in particles/cm^3 (averages and abrupt changes as defined above).

$\overline{V}$, δV: solar wind bulk speed in km/sec.

Time Resolution

The magnetometer data of the College, Alaska Observatory, and presumably the data of other magnetometer stations as well, have time errors of less than one minute. The A_E data, however, are based on 2.5-minute samplings of the magnetometer data [Davis and Sugiura, 1966]. The ATS 1 magnetometer data are available in the form of 2.5 minute averages, and the accompanying electron flux values are 6-minute averages. The Explorer 33 and 35 magnetometer data, plotted at one-minute intervals, represent 82-second averages [Ness et al., 1967]. Solar wind parameters are measured by the Explorer plasma instruments once every 2.7 minutes [Howe et al., 1971], although in some cases only hourly averages of the plasma data were on hand. The original data plotting scales generally allowed the above times to be read with an accuracy of about ±2 minutes.

Data Measurement Errors

Data errors are relatively difficult to ascertain. For the parameters

of primary concern, those involving magnetic fields, we suspect that the measurement errors are generally no greater than the reading errors, particularly where the parameter is defined in terms of a change in magnetic field. Magnetic field reading errors are approximately as follows: for surface data, ±2γ (±10γ for A_E data), for ATS 1 data, ±1γ, and for Explorer 33 and 35 data, ±0.25γ and ±5°.

The parameter $\Delta H_{ATS} = H - \overline{H_{QQ}}$ is subject to greater uncertainty because (1) the determination of $\overline{H_{QQ}}$ involves an uncertainty of perhaps 5-10γ, and (2) pre-sc values of H may contain a compressional enhancement which is not reflected in the very quiet non-storm-time conditions under which $\overline{H_{QQ}}$ is determined. The latter source of error should result in somewhat inflated values of ΔH, particularly on the day side of the magnetosphere.

Data Tabulation

The parameters described above are tabulated for each of the 37 sudden commencement events in Tables 3 through 7. The parenthesized solar wind values are based on hourly averaged data. The particular Explorer satellite or satellites used to supply data for a given sudden commencement event depended on such factors as satellite launch date, position in space, and data recording or transmitting gaps. The insets at the top of Figures 2 and 5 show the projections in the ecliptic plane of the positions of the satellites used to acquire the accompanying data.

DATA ANALYSIS

The aim of the analysis is, first, to determine what constitutes an sc event in terms of data variations in interplanetary space, in the magnetosphere, and at the earth's surface, both at and near the time of the sc. Then we attempt to determine the particular conditions under which some sc's signal the onset or intensification of magnetic bay activity, and to also identify some of the magnetospheric manifestations of such activity.

General Parameter Behavior

1. Behavior Simultaneous with Sc's

a. Interplanetary Space

Data observed simultaneous with sc's reveal that an abrupt increase in the IMF magnitude, B, is typically associated with the sudden commencement. B enhancements were observed in 31 of the 34 cases for which such data were available, with values ranging up to 14γ. However, in one case (4-23-67) B did not change and in two others B decreased by 3γ (11-3-67) and 4γ (7-3-68). Abrupt changes in IMF direction angles, ϕ and θ, also often occur simultaneously with the sc's. These changes have no clearly preferred direction and, here, range as high as 210° for ϕ and 105° for θ. It is well known that these sc-associated IMF variations are produced by interplanetary discontinuities imbedded in the solar wind. The simultaneity of these discontinuities with the sc's is only evident when allowance is made for the position in space of the observing satellite and the speed of the solar wind. In passing, we note that discontinuities are categorized as either rotational or tangential. The 34 sudden commencements with adequate

IMF coverage involve 23 rotational discontinuities ($\delta\theta \leq 10°$ and $\delta B < 1\gamma$), and 1 non-discontinuity ($\delta\theta = 0$ and $\delta B = +1\gamma$). The IMF discontinuities in Figure 2 might be classified as weak rotational discontinuities, even though the case of 29 NOV features a strong tangential component.

Abrupt changes in solar wind density (N) and bulk speed (V) also tend to occur simultaneous with sc's. As would be expected, the observed changes are consistently positive for both N and V, ranging up to $+14/cm^3$ and +150 km/sec.

b. Magnetosphere (ATS 1)

Abrupt increases in the magnetospheric horizontal magnetic field component, H, also typically accompany sc's. Of the 23 sc's for which ATS 1 magnetic field data were available and not associated with unduly strong pre-sc activity, 17 exhibit a simultaneous H variation, one of which (2-7-67) appears to be negative. Five other enhancements occur within ten minutes of sc's. The strongest enhancement (δH_{ATS}) is $+63\gamma$ on 2-15-67. Changes in the D and V magnetic field components include strong local time effects and are much less systematic.

Sc-simultaneous compressional effects are also common in the case of 50-150 keV electron flux. This parameter exhibited such enhancements (using 6-minute flux averages) in 12 of the 15 cases for which data was on hand, although 3 of these 12 enhancements were probably influenced by pre-sc activity. Two of the three remaining cases showed an increase within about 10-15 minutes of the sc. Higher-energy electron flux changes simultaneous with the sc's are generally positive but quite small.

c. Ground

The low-latitude magnetic signature of the sc is an abrupt enhancement (δH_{SFC}) of the horizontal component. This is simultaneous with the sc (indeed, such enhancements are the basis for sc observations) and the averaged magnitudes observed here range from +3γ to +56γ.

The high-latitude magnetic signature of the sc is more variable than the low-latitude signature. In these 37 cases, it was sometimes altogether absent (3 cases) and sometimes masked by superimposed activity (4 cases). On the other hand, the signature may consist of a limited enhancement, including discrete spikes, (10 cases), or more commonly an abrupt onset (11 cases) or intensification (9 cases) of magnetic bay activity. These sc-simultaneous magnetic bay enhancements are generally no stronger than 200γ, although more intense enhancements often follow.

2. Behavior Before and After Sc's

a. Interplanetary Space

The IMF magnitude is usually weak (5-10γ) and stable before the sc and strong (>10γ) and disturbed following it. The IMF direction behaves less predictably, although it sometimes becomes more disturbed after the sc. The major changes in IMF direction are not always simultaneous with the sc, sometimes occurring shortly before or after it. Even a large part of the sc-magnitude change may follow the sc by several minutes. These IMF changes are frequently sustained for a prolonged period.

Many sc events are very clearly marked in the solar wind, with few large preceding or following fluctuations. However, solar wind density and bulk speed tend to display more extreme fluctuations before and after the sc

than does the frozen-in magnetic field.

b. Magnetosphere (ATS 1)

Large-scale variations of the magnetic field and electron flux at ATS 1 are known to have a pronounced diurnal component. Other pronounced, large-scale variations of these parameters, associated with plasma inflation and acceleration processes, frequently alter the quiet-time, diurnal variations. Many sc-associated variations (H enhancements) appear to be merely superimposed on the above, but others (H depressions) appear to be identified with some of the large-scale variations themselves.

Increases in the horizontal component of the magnetic field occur in 22 of the 23 cases for which such data were available and not dominated by pre-sc activity. These enhancements are often sustained for an hour or more before subsiding (10 cases). Frequently, however, a depression begins within a few tens of minutes after the sc (12 cases). These post-sc declines tend to be quite rapid and are commonly much more extensive than a simple recovery of the sc-associated enhancement. This is observed in 10 of the 16 cases in which post-sc declines occurred. In three of the remaining six cases, rapid and extensive H declines occurred within about 2 hours after the sc-enhanced field recovered.

We have seen that the 50-150 keV electron flux commonly exhibits sc-associated enhancements similar to those of H. The data shows that the post-sc declines of this parameter are likewise similar to those of H. As for the 150-500 keV and 500 keV-1 MeV electron fluxes, whose sc-associated increases tend to be weak or non-existent, their post-sc declines begin concurrent with or sooner than those of H or low-energy electron flux. This

behavior is clearly illustrated in Figure 5. Even though this event features an intense pre-sc activity enhancement just minutes before a moderately strong sc, the decline of high-energy electron flux begins almost immediately after the sc.

c. Ground

The three low-latitude magnetometer stations (Honolulu, San Juan, and Tashkent) were used primarily to estimate the magnitude of the sudden commencements. These stations are situated close enough to the orbital plane of ATS 1 that their H-component traces are somewhat similar to that of ATS 1. That is, the abrupt magnetic field enhancement that marks the sc is apparent at these stations as well as at ATS 1, and it is often followed by a likewise-simultaneous field depression onset.

Geomagnetic activity before and after the sc at high-latitude stations is quite variable. Preceding activity may be nonexistent, or it may be strong and erratic enough to prevent the certain identification of an sc-associated enhancement. Subsequent activity may also be non-existent, or it may soon intensify into a major disturbance.

Many aspects of general parameter behavior, as well as some distinguishing aspects of sc-related bay enhancements, are illustrated in Figures 2 through 7. Figures 2 through 4 compare an sc event associated with a simultaneous auroral-zone magnetic bay onset (13 SEP 67) with one lacking such an enhancement (29 NOV 67). Figure 2 shows that the sc is well-marked in the solar wind velocities of both events. Although the IMF magnitude increase is stronger in the case of 29 NOV, its effect is to make the vertical IMF component, B_Z, more positive, while the increase of 13 SEP acts to make

B_Z more negative. Figure 3 shows intense magnetic field and particle flux depressions occurring soon after the compressional increase of 13 SEP, and Figure 4 shows sc-simultaneous bay onsets occurring at two auroral-zone stations on that date. No sc-simultaneous auroral-zone bay onset is observed on 29 NOV, although a slowly developing bay did begin at the polar cap station, VOSTOK.

Figure 5 indicates an sc-associated interplanetary discontinuity at about 1625, when EXPLORER 33 is 60 R_E sunward of the earth. The indicated solar wind speed behind the discontinuity is about 550 km/sec, which agrees well with a 1636 sudden commencement time. However, the ATS 1 electron flux data show a strong disturbance beginning somewhat before 1636, following over an hour of southward IMF and declining H_{ATS} and low-energy electron flux. This is consistent with the pre-sc A_E activity shown in Figure 6, climaxed by the strong sc-masking increase beginning near 1615. Note that the A_E profile is a composite of the A_U and A_L profiles, which are derived from the more prominent features of the magnetogram profiles shown on the left.

Figure 7 presents the sc event of 1 APR 67. Like the case of 13 SEP 67, this event features an sc-simultaneous bay onset in the presence of an uninflated magnetosphere (see NO-YES category, Table 4). The sc magnitude is indicated here by the sudden magnetic field enhancement at Honolulu, one of the three low-latitude stations used to compute $\overline{\delta H_{SFC}}$. The sc is accompanied by a sharp intensification of negative B_Z, produced primarily by an abrupt decrease of θ from near 0° to about -60°. At ATS 1, pre-sc H is only slightly below quiet-time ($\overline{H_{QQ}}$) values. The weak 0807 compressional in-

crease in H is followed at 0820 by the onset of a vigorous depression. A compressional increase is also apparent in the two lower-energy electron flux channels, but an immediate depression onset occurs in the high-energy channel. This is consistent with the usual pre-midnight (local time) decrease of trapped high-energy electron flux in response to a magnetospheric substorm [Lezniak and Winckler, 1970]. However, note that a substantial particle "drop-out" occurs here in less than 10 minutes.

Having completed this general overview of sc-associated variations, we wish to examine the interrelationships between the parameters involved, both at and near sc's, in an attempt to identify the conditions under which an sc will signal the onset or intensification of a polar magnetic bay.

Conditions Associated with Sc-related Magnetic Bay Enhancements

The data indicate that 20 of the 37 sc's are clearly associated with simultaneous, abrupt onsets or intensifications of high-latitude magnetic bay activity. This activity, produced by the auroral electrojet, is measured in terms of the time profile of the A_E index. We have also examined the associated A_U and A_L profiles and individual magnetograms in order to clarify or supplement the A_E profiles. For example, in cases where the sc-simultaneity of an A_E enhancement was in doubt, as for the sc's of 5-25-67 and 2-10-68, the individual magnetograms were examined.

We now attempt to organize the data in such a way that the relationship of auroral electrojet activity to sc-associated magnetospheric and interplanetary conditions is clarified. To do this, we categorize these events according to the behavior of A_E activity at and near the sc's. This

categorization is accomplished by the application of two qualitative criteria, (1) the existence of pre-sc A_E activity and (2) the occurrence of an abrupt, sc-simultaneous enhancement of extended A_E activity. The condition on the first criterion is merely that the A_E activity preceding the sc should not be negligible (near zero). The condition on the second criterion is that the enhancement must consist of a bay-like development (as opposed to a discrete spike) or, in the case of newly developing activity, vigorous bay development must begin within a very short time (~10 minutes) after a weak sc-simultaneous A_E enhancement.

According to how criteria (1) and (2) are satisfied, these cases are divided into four categories: YES-YES, NO-YES, YES-NO, and NO-NO, where, for example, the NO-YES category includes cases without pre-sc activity but with an sc-simultaneous bay onset. In Tables 3 through 6 we list the events by category and tabulate the surface, magnetospheric, and interplanetary-space parameters for each. Table 7 includes the four cases for which determination of the occurrence of an sc-simultaneous enhancement has been prevented by the masking effect of strong A_E activity already underway.

We now compare the behavior of the various parameters tabulated here, from the standpoint of the four categories of A_E activity listed above. For convenience, these comparisons rely mainly on the use of the data averages shown under each data column in the Tables. When an average is given, the number of cases used to compute the average is shown. Where the average appears to be misleading it is so stated. Also, the occurrence of extremely atypical cases will be identified.

We realize that some aspects of the analysis suffer because of the lim-

ited number of cases studied. Missing data is also a problem, especially where the solar plasma parameters are concerned. Therefore, even though an attempt will be made to identify any patterns appearing in the data, such patterns will not be considered as findings when based on just a few cases.

Comparison of the parameters by category yields the following results:

$\overline{V}$, $\overline{N}$: For the limited solar wind data presented here, cases exhibiting prior A_E activity tend to have enhanced pre-sc solar winds, in either velocity or density. Specifically, the sc's associated with simultaneous bay enhancements (YES-YES) tend to exhibit high $\overline{V}$ and low $\overline{N}$ ($\overline{\overline{V}}$ = 550 km/sec and $\overline{\overline{N}}$ = 1.6/cm^3 for 3 cases), whereas those not associated with simultaneous bay enhancements (YES-NO) tend to exhibit high $\overline{N}$ and low $\overline{V}$ ($\overline{\overline{N}}$ = 7.9/cm^3 and $\overline{\overline{V}}$ = 390 km/sec for 4 cases).

δV, δN: For categories with an sc-simultaneous bay enhancement the simultaneous solar wind speed enhancement tends to be large ($\overline{\delta V}$ = +90 km/sec for 1 YES-YES case and +99 km/sec for 6 NO-YES cases). Thus, for the solar wind data presented here, cases exhibiting sc-simultaneous bay enhancements tend to be associated with higher pre-sc solar wind speeds and/or higher simultaneous solar wind speed enhancements than do cases lacking the bay enhancements.

$\overline{\delta H_{SFC}}$: The cases with no A_E activity at all, either prior to or commencing at the sc, tend to have weaker simultaneous enhancements of low-latitude magnetic field than do cases falling in the other categories ($\overline{\overline{\delta H_{SFC}}}$ = +12.7γ for 9 NO-NO cases as opposed to +21.4 ± 1.0γ for 24 other cases), where $\overline{\delta H_{SFC}}$ is a longitudinally averaged parameter related to sc magnitude. This finding is consistent with the above solar wind values, in that this is

the only category exhibiting neither enhanced pre-sc solar wind (speed or density) nor strong, simultaneous solar wind speed enhancements. Note, however, that the weakest $\overline{\delta H_{SFC}}$ of all ($\overline{\delta H_{SFC}} = +3\gamma$) occurs in the NO-YES category.

δH_{ATS}: This parameter is similar to $\overline{\delta H_{SFC}}$ in its relationship to sc magnitude. Here, too, cases with no activity at all (NO-NO) tend to have weaker values than the other three categories. However, the average δH_{ATS} in these other categories is not uniformly high, in contrast to the averaged values of $\overline{\delta H_{SFC}}$. A related feature of the data is that δH_{ATS} values are often quite different from the accompanying $\overline{\delta H_{SFC}}$ values, both by case and by category.

ΔH_{ATS}: This parameter represents the departure of H_{ATS} from its quiet-time value, in this case at t_{sc}, just before the abrupt enhancement occurs. Negative values of this parameter correspond to depressed values of H_{ATS} and generally are accompanied by enhanced geomagnetic activity. For all categories but YES-YES, average values indicate quiet-time conditions ($\overline{\Delta H_{ATS}} = 1\gamma \pm 3\gamma$ for 17 cases). However, for YES-YES cases the average value is appreciably depressed ($\overline{\Delta H_{ATS}} = -20\gamma$ for 7 cases).

Magnetospheric depressions and recoveries: In addition to the magnetospheric parameters already discussed, the data tables also contain remarks regarding significant changes in the behavior of H and J (electron flux) at and near t_{sc}. The cases with sudden bay enhancements are differentiated from the rest by the fact that a majority of those with magnetospheric data exhibit H and/or J depressions at or within a few tens of minutes after t_{sc} (9 out of 14 YES-YES and NO-YES cases as opposed to 2 out of 11 NO-NO and YES-

NO cases). These depressions occur in all four quadrants of the ATS 1 orbit, although a greater number is observed in the evening quadrant (04-10 UT). The 4 cases exhibiting H and/or J recoveries occurred only in categories featuring pre-sc activity followed by either identifiable sc-simultaneous bay enhancements (1 YES-YES case) or by continuing vigorous activity (3 MASKED cases).

$\overline{B}$, $\overline{\phi}$, $\overline{\theta}$, $\overline{B_Z}$: The average IMF magnitude for the preceding half-hour, $\overline{B}$, is somewhat enhanced for the categories exhibiting prior activity ($\overline{\overline{B}}$ = 8.8γ for 8 YES-YES cases and 9.0γ for 3 YES-NO cases as opposed to 5.8γ for 10 NO-YES cases and 5.9γ for 9 NO-NO cases). This is consistent with the enhanced pre-sc solar wind values observed in the prior-activity categories.

The parameter $\overline{\phi}$ is much the same for the YES-YES ($\overline{\overline{\phi}}$ = 168° for 8 cases) and the NO-NO ($\overline{\overline{\phi}}$ = 193° for 9 cases) categories. Thus, this parameter has no apparent significance as far as pre-sc or sc-associated A_E activity is concerned.

The parameters $\overline{\theta}$ and $\overline{B_Z} = \overline{B}\sin\overline{\theta}$, unlike $\overline{\phi}$, discriminate clearly between the YES-YES and NO-NO categories, with moderately negative values for YES-YES ($\overline{\overline{\theta}}$ = -22° and $\overline{\overline{B_Z}}$ = -2.4γ for 8 cases) and moderately positive values for NO-NO ($\overline{\overline{\theta}}$ = +28° and $\overline{\overline{B_Z}}$ = +2.9γ for 9 cases). These parameters have average values near zero for the other two categories, these averages representing a balance between generally moderate positive and negative values. Note that the only category to exhibit appreciably negative $\overline{\overline{\theta}}$ and $\overline{\overline{B_Z}}$ (YES-YES) is also the only category to exhibit appreciably negative $\overline{\overline{\Delta H_{ATS}}}$. Also, note that $\overline{\overline{\Delta H_{ATS}}}$ is near zero whether $\overline{\overline{\theta}}$ and $\overline{\overline{B_Z}}$ are near zero (NO-YES, YES-NO) or moderately positive (NO-NO).

δB, $\delta\phi$, $\delta\theta$, δB_Z: The sc-simultaneous IMF magnitude enhancement, δB, has a somewhat greater average value for the YES-YES category ($\overline{\delta B} = +8.5\gamma$ for 7 cases) than for the other categories ($\overline{\delta B} \tilde{=} +4.7 \pm 0.3\gamma$ for 22 cases). It would be of interest to see if the YES-YES category has a correspondingly enhanced δV. However, limited solar wind data for this category precludes this. Note, also, that the cases of 4-23-67 and 11-3-67 exhibit $\delta B \lesssim 0$.

The parameter $\delta\phi$ has a tendency to be positive for cases involving sc-simultaneous bay enhancements ($\overline{\delta\phi} = +23°$ for 7 YES-YES cases and $+40°$ for 10 NO-YES cases) and negative for the other categories ($\overline{\delta\phi} = -13°$ for 3 YES-NO cases and $-18°$ for 9 NO-NO cases).

The parameter $\delta\theta$ tends to be negative for the NO-YES category ($\overline{\delta\theta} = -22°$ for 10 cases) and positive for the NO-NO category ($\overline{\delta\theta} = +13°$ for 9 cases). This parameter is weakly positive for the remaining categories, due in the YES-YES category to the effect of a single strong increase in θ. The parameter δB_Z is usually negative for both the NO-YES cases ($\overline{\delta B_Z} = -4.2\gamma$ for 10 cases) and the YES-YES cases ($\overline{\delta B_Z} = -1.1\gamma$ for 7 cases), in spite of positive $\overline{\delta\theta}$ for the YES-YES. The latter behavior is due to the overshadowing effect of strongly positive $\overline{\delta B}$ in the presence of negative $\overline{\theta}$. The comparatively weak negative value of $\overline{\delta B_Z} = -1.1\gamma$ for the YES-YES category is due to the occurrence of a single strongly positive δB_Z on 1-13-67. Appreciably positive δB_Z is generally observed for the remaining cases ($\overline{\delta B_Z} = +4.0\gamma$ for 3 YES-NO cases and $+3.6\gamma$ for 9 NO-NO cases). It is clear from the data that the parameter δB_Z has the ability to discriminate between most cases exhibiting simultaneous bay enhancements and those exhibiting none.

In the NO-YES category this ability is characterized by the tendency of δB and $\delta\theta$ to work together to produce or enhance a negative B_Z, whereas in the YES-YES category this discriminatory ability of δB_Z is characterized by the tendency of δB to enhance an already existing negative B_Z. Note that the other distinguishing characteristic of these two categories is the common tendency to exhibit H_{ATS} and/or J_{ATS} depression onsets shortly after these abrupt sc-simultaneous B_Z decreases.

In cases where $\delta B_Z \tilde{=} 0$, the value of ΔH_{ATS} may be particularly significant. Specifically, the two cases of $\delta B_Z = 0$ in the YES-YES category (characterized by appreciably negative values of ΔH_{ATS}) are associated with bay enhancements, whereas the three cases with $\delta B_Z \tilde{=} 0$ in the NO-NO category (accompanied by slightly positive values of ΔH_{ATS}) are associated with non-occurrences.

DISCUSSION

The stratification of cases according to the occurrence of pre-sc A_E activity and sc-simultaneous bay enhancements (onsets and intensifications) appears to have been effective in organizing the data. Thus, many relationships became apparent that were not so clearly evident in the unstratified data.

As previously stated, the IMF data in this study are presented in the coordinate system in which they were made available, namely the Geocentric Solar Equatorial coordinate system (IMF data for 1-7-67 are in the Geocentric Solar Ecliptic system). Although it has been shown that the Geocentric Solar Magnetospheric system is somewhat more effective in describing the relationship between B_Z and geomagnetic activity [Hirshberg and Colburn, 1969], this study is not based on the close examination of specific values of B_Z. This study is based primarily on general comparisons between categories of events, where categories are defined independently of B_Z. The IMF parameter examined in most detail is δB_Z, whose relationship to geomagnetic activity appears to be independent of the coordinate system used [Meng et al., 1973].

Conditions for Triggering Sc-associated Magnetospheric Substorms

A primary finding is that the YES-YES category of sc-simultaneous bay intensifications and the NO-YES category of bay onsets are distinguished from the two non-occurrence categories by sc-simultaneous variations of the parameter B_Z. The variations tend to be negative for the bay occurrences and positive for the non-occurrences, indicating that the production or intensification of negative B_Z (southward IMF) is of central importance to the

occurrence of sc-associated bays, as it has been shown to be for other bays. It should be pointed out that the occurrence of a strongly positive δB_Z for the 1-13-67 YES-YES event does not detract from the indicated significance of negative δB_Z. This case is associated with the observation, near local midnight, of the abrupt recovery of a strongly depressed nightside magnetic field, indicating a substorm expansion onset. Other workers have also related the triggering of a substorm expansion, following prolonged magnetospheric inflation, to a sudden change of IMF direction from south to north [Aubrey and McPherron, 1971; Kokobun, 1971; Roederer, 1974]. This merely indicates that positive as well as negative δB_Z can be meaningfully correlated with bay enhancements in the YES-YES category.

This apparent significance of negative δB_Z is enhanced by the finding that the sc-simultaneous bay onsets occur under pre-sc magnetospheric and interplanetary conditions quite different from the bay intensifications. In fact, the pre-sc conditions for the bay onsets are similar to those of the two non-occurrence categories, in that neither $\overline{B_Z}$ nor $\overline{\Delta H_{ATS}}$ is appreciably negative. This clearly indicates that sc-simultaneous bay onsets can occur when the near nightside magnetic field has a dipole-like (uninflated) configuration. A random check of these cases discloses that they do indeed exhibit the particle precipitation and magnetic micropulsation activity that, together with the basic auroral electrojet enhancement, characterize typical magnetospheric substorms.

The indication that this class (NO-YES) of substorms occurs in the presence of an uninflated nightside magnetosphere is basic to an understanding of the role of sudden commencements in magnetospheric substorm trig-

gering. In the absence of readily available plasma in the form of a dipole-penetrating plasma sheet, other means of plasma supply must be considered. Four means of supply that might be invoked are (1) direct precipitation of particles already trapped on the high-latitude dipole field lines, (2) precipitation of plasma-sheet particles suddenly available to these field lines following their tailward distention (at Alfvén speed) in response to an abrupt dawn-dusk plasma sheet current enhancement associated with the sc-simultaneous production or intensification of southward IMF noted above, (3) precipitation of plasma-sheet particles suddenly available to these field lines due to rapid convection of the plasma sheet into the inner magnetosphere from the magnetotail in response to an abrupt dawn-dusk magnetospheric electric field enhancement associated with the southward IMF enhancement noted above, and (4) precipitation of particles suddenly available to these field lines following turbulent transport of particles from the magnetopause or polar cleft in response to enhanced solar wind particle penetration into the dipole, associated with enhanced field-line merging accompanying the southward IMF enhancement noted above.

Minimum time scales pertaining to these particle supply mechanisms might be on the order of (1) a few seconds for direct precipitation, (2) a few minutes for sheet-current enhancement and Alfvén-speed field line distention, (3) a few tens of minutes for magnetospheric electric field enhancement and plasma sheet convection from the magnetotail, and also (4) a few tens of minutes for solar-wind particle penetration and turbulent transfer from the magnetopause or polar cleft. The last two mechanisms are considered less likely to be involved because of their comparatively long time

scales. However, the first and second mechanisms may apply. The direct precipitation of particles already trapped on high-latitude field lines is presumably triggered by the sc-simultaneous magnetospheric compression. The triggering mechanism might be non-adiabatic, requiring the generation of an instability [Parks et al., 1972; Perona, 1972], or it might be adiabatic, as in the sudden lowering of particle mirror points by magnetospheric compression [Swift, 1965; Lin et al., 1974]. It should be pointed out that the feedback mechanism between electrostatic and electromagnetic waves proposed by Parks would not apply to the generation of substorms in the presence of an uninflated magnetosphere. However, it is possible that feedback from ionosphere to magnetosphere might occur due to the increased ionospheric conductivity which would result from the lowering of trapped-particle mirror points to ionospheric heights. The foregoing compressional, direct-precipitation mechanism, in combination with the δB_z-related mechanism of sudden tailward dipole-distention might help to account for both the immediate precipitation response and the sustained particle supply that are typical of sc-associated substorms.

Magnetospheric compression and a sudden decrease in B_z are also observed in cases of the YES-YES category, characterized by a somewhat inflated magnetosphere. For these cases, the process of enhanced earthward plasma sheet convection, listed above, may be included with magnetospheric compression and field-distention in possible sc-associated bay-intensification mechanisms. On the other hand, this category also includes cases where other substorm-producing mechanisms may be involved, as in the case of 1-13-67, where a strongly positive δB_z may have been associated with the abrupt re-

covery of the nightside field to a more dipole-like configuration, or the cases of 1-7-67 and 5-25-67, where $\delta B_Z \approx 0$. Thus, the possible substorm-producing mechanisms at work in the YES-YES category are too numerous and uncertain to effectively analyze using the data at hand.

Underscoring the probable involvement of the magnetospheric compressions in most of these sc-associated substorm triggerings is the fact that the sc amplitude, $\overline{\delta H_{SFC}}$, shows a strong tendency to be large for these events. In spite of this tendency, the data do not indicate that this parameter either adds to or detracts from the effectiveness of δB_Z in determining whether or not these substorms occur. For example, a substorm onset occurred on 4-23-67 accompanied by $\delta B_Z = -14\gamma$, even though the sc-amplitude was just 3γ, the lowest of all 37 cases. Alternatively, although no substorms occurred in conjunction with the three next-lowest sc amplitudes (each 6γ), the accompanying values of $\delta B_Z \tilde{=} 0$ (NO-NO category) were themselves consistent with these non-occurrences.

Effectiveness of the Parameter ΔH_{ATS}

The parameter ΔH_{ATS} appears to be a reasonably effective indicator of pre-sc magnetospheric inflation, in spite of the uncertainties involved in its determination and its observed tendency to exhibit negative values on the night side of the ATS 1 orbit (see Figure 10). The categories in which this tendency is strongest are the NO-NO, YES-NO, and MASKED. Of the remaining fourteen events for which ATS 1 data were available, appreciably negative values of ΔH_{ATS} were observed in all seven YES-YES cases, even though the satellite was well on the day side of the magnetosphere in three of these

cases. On the other hand, the lack of appreciable pre-sc inflation was indicated for all seven NO-YES cases, even though the satellite was on the night side in three of these cases and near dawn or dusk in four cases.

Comparison of Sc-associated Substorms with Other Substorms

This study presents further evidence that important similarities can exist between sc-related substorms and other substorms. As stated earlier, sc-associated substorms appear to have the same general precipitation, auroral-electrojet, and magnetic micropulsation characteristics as other substorms. In addition, some of the magnetospheric and interplanetary variations that tend to accompany sc-associated substorms have been observed in conjunction with other substorms as well. For example, sc-related bay enhancements tend to be followed by depressions of magnetic field and electron flux at ATS 1. In the case of 4-1-67 (Figure 7), the onset of a high-energy electron flux drop-out was essentially simultaneous with the local-evening sc, with magnetic field and low-energy electron flux depressions beginning 13 minutes later. Local-evening energetic electron flux drop-outs and accompanying magnetic field decreases have also been observed at synchronous orbit during non-sc substorms, and for isolated substorms the drop-outs have nearly coincided with the onsets of A_E activity [Lezniak and Winckler, 1970; Erickson and Winckler, 1973]. These particle drop-outs are apparently adiabatic effects, since the trapped energetic electrons have a drift time which is short in comparison with the substorm period. Thus, the drop-outs appear to represent a sudden redistribution of particle drift shells in the magnetosphere, i.e., a sudden change to a more tail-like magnetospheric configura-

tion.

Another phenomenon common to some sc - and non-sc - related substorms is the sudden enhancement of southward IMF. For sc-related substorms, this usually occurs simultaneous with the substorm onset by means of some combination of enhanced IMF magnitude and enhanced southward direction. For other substorms (e.g., see the events of 0740 on 11-29-67 in Figures 2-4 and 1520 on 2-7-67 in Figures 5-6), this enhancement of southward IMF results from a southward turning and usually precedes the substorm onset by several minutes [Tsurutani and Meng, 1972; Meng et al., 1973].

Thus, sudden enhancement of southward IMF, local-evening adiabatic electron flux drop-outs and accompanying magnetic field decreases, and abrupt onset of auroral-zone electron precipitation, are sometimes observed in both sc- and non-sc related substorms. It is possible that the interplanetary discontinuity is the cause of the magnetospheric and ionospheric disturbances, perhaps by the dipole-distending mechanism discussed earlier. Whatever the mechanisms may be, the findings indicate that they are able to produce an abrupt substorm onset associated with a rapid change in the configuration of an uninflated magnetosphere.

SUMMARY

This analysis of 37 sudden commencement events categorized on the basis of pre-sc activity and sc-simultaneous substorm occurrence, indicates that pre-sc magnetospheric inflation is not a necessary condition for the occurrence of sc-related substorms. Likewise, there was no evidence that strong sc amplitude is essential for the triggering of these substorms. Most sc-related bay onsets or intensifications were accompanied by the onset or intensification of southward IMF, whereas most non-occurrences featured a change to a more northward IMF.

Some of these sc-related substorm onsets were observed to be associated with adiabatic drop-outs of magnetospheric electron flux and accompanying magnetic field decreases, at synchronous orbit. These appear to represent a sudden change to a more tail-like magnetospheric configuration.

Thus, the data indicate that sc-related substorms can begin in conjunction with sudden enhancement of southward IMF and abrupt change of a dipole-like nightside magnetic field to a more distended configuration. A cause-effect relationship between these phenomena is a possibility discussed here, but this has not been established. Furthermore, it is not suggested that all sc-related substorms occur in this way. For example, one contrasting substorm event features a sudden onset of northward IMF, associated with an abrupt change of a tail-like nightside magnetic field to a more dipole-like configuration. Both processes appear to be possible and justifiable.

Finally, these types of sc-substorm-related variations have also been observed in connection with other substorms, suggesting that similar mechanisms can be involved in both sc - and non-sc - related substorms.

SUGGESTIONS FOR FURTHER RESEARCH

This study represents an initial attempt to determine some of the conditions under which magnetospheric substorms occur. Sc-associated substorms were selected for study because the associated interplanetary, magnetospheric, and ionospheric disturbances are well-marked. The analysis relies heavily on the categorization of a limited number of sudden commencement events according to particular sequences of A_E activity. A definitive treatment of this problem would require many more events in each category than are presented here.

Particular attention needs to be given to the relationship of the solar wind plasma parameters to the sc-associated enhancements and to the pre-sc conditions of both the IMF and the auroral electrojet. Several interesting relationships were suggested by the data, but complete data were not available for many events.

Another promising subject for investigation might be the comparison of sc-amplitudes observed at the ground ($\overline{\delta H_{SFC}}$) with those observed at synchronous orbit (δH_{ATS}). Preliminary work suggests that synchronous amplitudes are significantly less than surface amplitudes for sc-related substorm events occurring during local nighttime, and that this nightside δH_{ATS} deficit may be partly a function of the parameter δB_Z, as opposed to being a purely diurnal effect. If so, this might indicate the effects at synchronous orbit of the dawn-dusk plasma sheet current discussed earlier in connection with δB_Z.

It is also important to obtain and study more magnetospheric particle data from geostationary satellites, including the complete set of distribu-

tion functions for the various particles, before, during, and after sc disturbances. These data are especially sensitive to magnetospheric disturbances and could be a most useful source of new information about particle precipitation mechanisms.

PLASMA ACCELERATION DUE TO $\partial B_x/\partial t$

Introduction

This study reaffirms the important relationship known to exist between the z-component of the IMF and substorm activity. The explanation for this relationship is generally believed to involve an enhanced dawn-to-dusk magnetospheric electric field, driving the plasma sheet earthward from the magnetotail. It was suggested earlier that an important related effect may be the enhanced dawn-to-dusk plasma sheet current, causing rapid distention of auroral-zone field lines tailward to the plasma sheet. Van Allen [1970] suggested that such magnetospheric effects of a negative B_z arise from the $\vec{V}x\vec{B}_z$-associated motional electromotive force (emf) generated by the movement of the IMF past the earth.

The possibility is raised here that a transformer emf might also be involved in motions of magnetospheric plasma. This emf would also arise from the movement of the IMF past the earth, but it would involve a time-changing x-component (earth-sun direction) and would act around the circumference of the magnetotail boundary layer rather than across the magnetotail. Briefly, the transformer emf would act around the magnetotail, as on a tightly-wound solenoid, in response to the limited radial penetration along the flanks of the magnetotail of a spatially varying, solar-wind-borne IMF. The solenoidal current generated by this emf would produce a transient magnetic field directed parallel to the axis of the magnetotail. This field would interact with the earth's magnetic field to produce a transient magnetic stress which could accelerate plasma sheet particles from the magnetotail into the local-midnight trapping zone, where precipitation could occur.

Description of the Acceleration Mechanism

The means by which an earthward nightside plasma acceleration might be produced by a transient magnetic stress resulting from variations in the x-component of the solar wind's frozen-in magnetic field will now be outlined. First, an electromagnetic interaction between the IMF and the magnetopause is postulated in terms of a transformer emf,

$$\varepsilon = \int_S \dot{B}_x ds,$$

induced on the magnetopause, around the circumference of the magnetotail in the yz plane by a penetrating, time-changing IMF. Here, $\dot{B}_x$ is the rate of change of the x component of the magnetic flux, in the frame of reference of the magnetopause, due to solar wind convection of a spatially varying, frozen-in IMF. We assume that some solar wind (and IMF) penetration of the magnetotail boundary layer occurs, and we take S to be the annular, cross-sectional area penetrated at any given distance tailward of the earth.

This emf might be capable of generating an electric current on the magnetopause in the plane of S by means of a non-collisional, turbulent conductivity based on wave-particle interaction [Coroniti, 1969]. We express the magnetopause current density as

$$j = -\sigma d \dot{B}_x,$$

where σ is the effective magnetopause conductivity and d is the depth of IMF penetration into the magnetotail boundary layer.

Since values of $\dot{B}_x$ are convected tailward, presumably at the speed of the solar wind, the associated transverse magnetopause current should take on the configuration of a solenoid. Then an axially directed magnetic field should be generated within this magnetospheric solenoid, whose value in the

near nightside magnetosphere is expressed as

$$B_1 = -\mu_0 \sigma d \delta \dot{B}_x/2,$$

where μ_0 is the permeability constant and δ is the magnetopause current depth.

We must now indicate how this transient magnetic field might accelerate magnetospheric plasma. Starting from the equation of motion for a fully ionized, current-carrying plasma,

$$\rho(\vec{dv}/dt) = -\nabla p + \vec{j}\times\vec{B},$$

we expand the last term,

$$\vec{j}\times\vec{B} = (\nabla\times\vec{B})\times\vec{B}/\mu_0.$$

Then the x-component of the resulting equation, neglecting the shear stresses but not the tension stress, becomes

$$\rho_x(\partial v_x/\partial t) = -\partial/\partial x[p + (B^2 - B_x^2)/2\mu_0],$$

with presumed application near the $z=0$ plane of the near nightside magnetosphere. Application of the kinetic energy theorem then leads to

$$v_1 = \sigma d \delta \sqrt{\mu_0/\rho_x}\, \dot{B}_x/2,$$

where v_1 is the transformer-emf-associated component of the axial velocity of magnetospheric plasma near the axis of the near nightside magnetosphere and ρ_x is the plasma mass per unit area in the x direction near the axis. Thus, a transient earthward plasma velocity component should be associated with positive interplanetary $\dot{B}_x$, due to changes in the magnitude of $\vec{B}$ and/or its longitudinal angle, ϕ.

Applicability of the Mechanism

A magnetospheric plasma acceleration mechanism is presently being sought

to explain the injection of discrete plasma clouds near the midnight meridian. One explanation assumes the existence of a transiently intensified electric field spatially confined to the vicinity of the midnight meridian [De Forest and McIlwain, 1971; Roederer and Hones, 1974]. An alternative explanation might be the generation of a transient magnetic stress near the magnetotail axis, as outlined above. It remains to be seen if these plasma injections can be associated with observations of positive interplanetary $\partial B_x/\partial t$.

FIGURE 1

DISTRIBUTION OF SC EVENTS
BY UNIVERSAL TIME &
LONGITUDE OF LOCAL MIDNIGHT

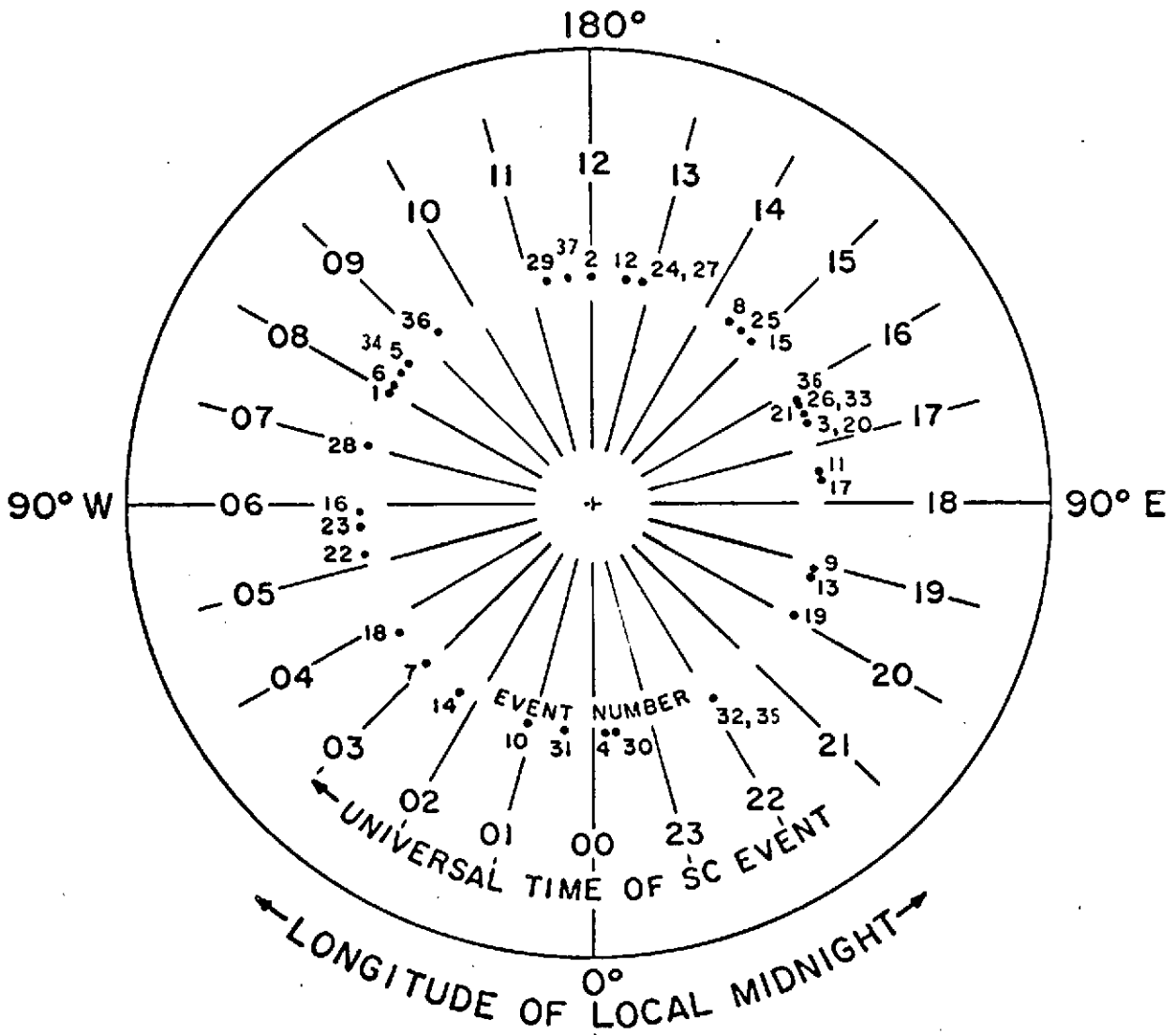

FIGURE 2

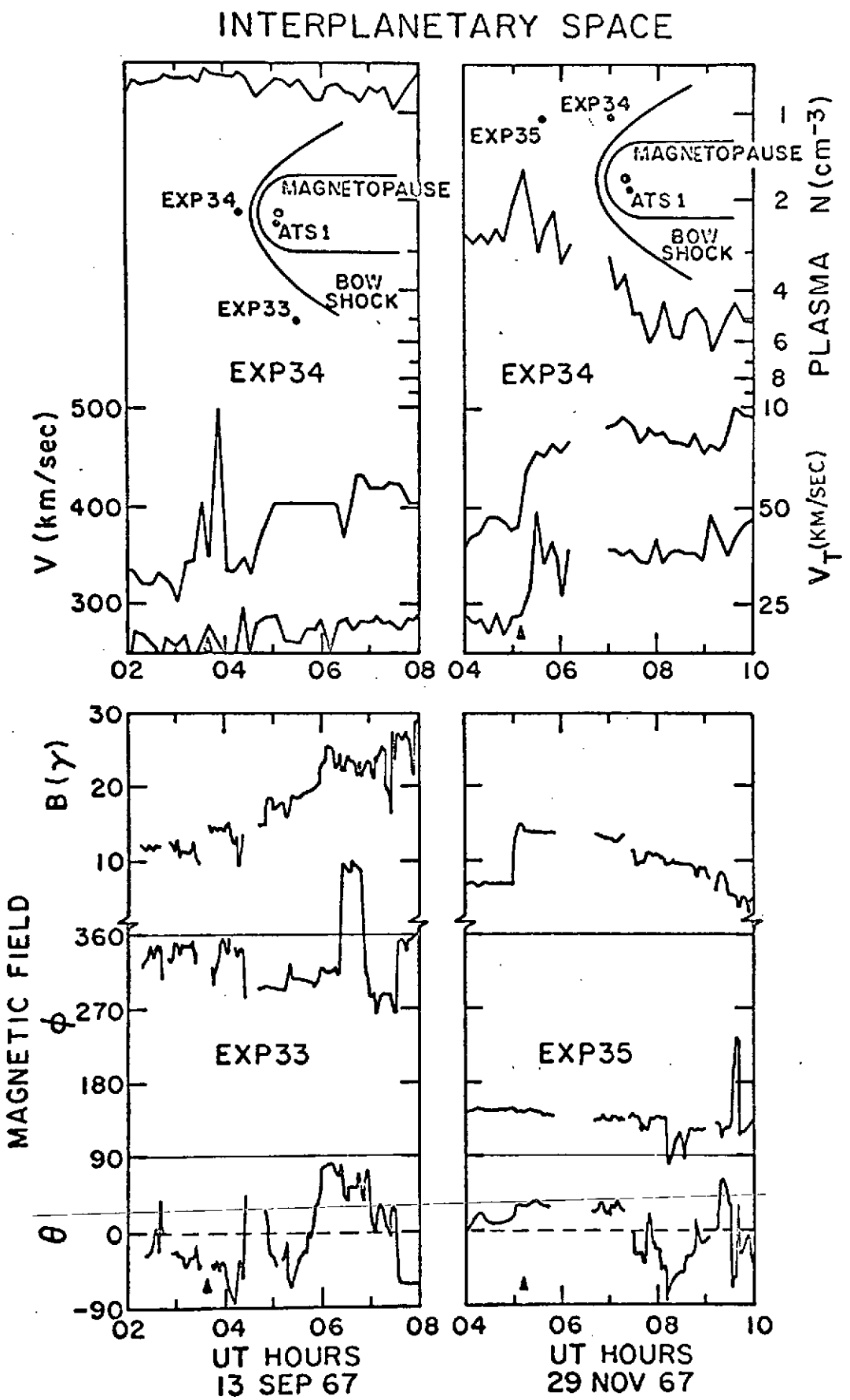
INTERPLANETARY SPACE
EXP34
MAGNETOPAUSE
ATS 1
BOW SHOCK
EXP33
EXP35
V (km/sec)
PLASMA N(cm-3)
V_T(KM/SEC)
MAGNETIC FIELD
B(γ)
φ
θ
02
04
06
08
10
UT HOURS
13 SEP 67
29 NOV 67

FIGURE 3

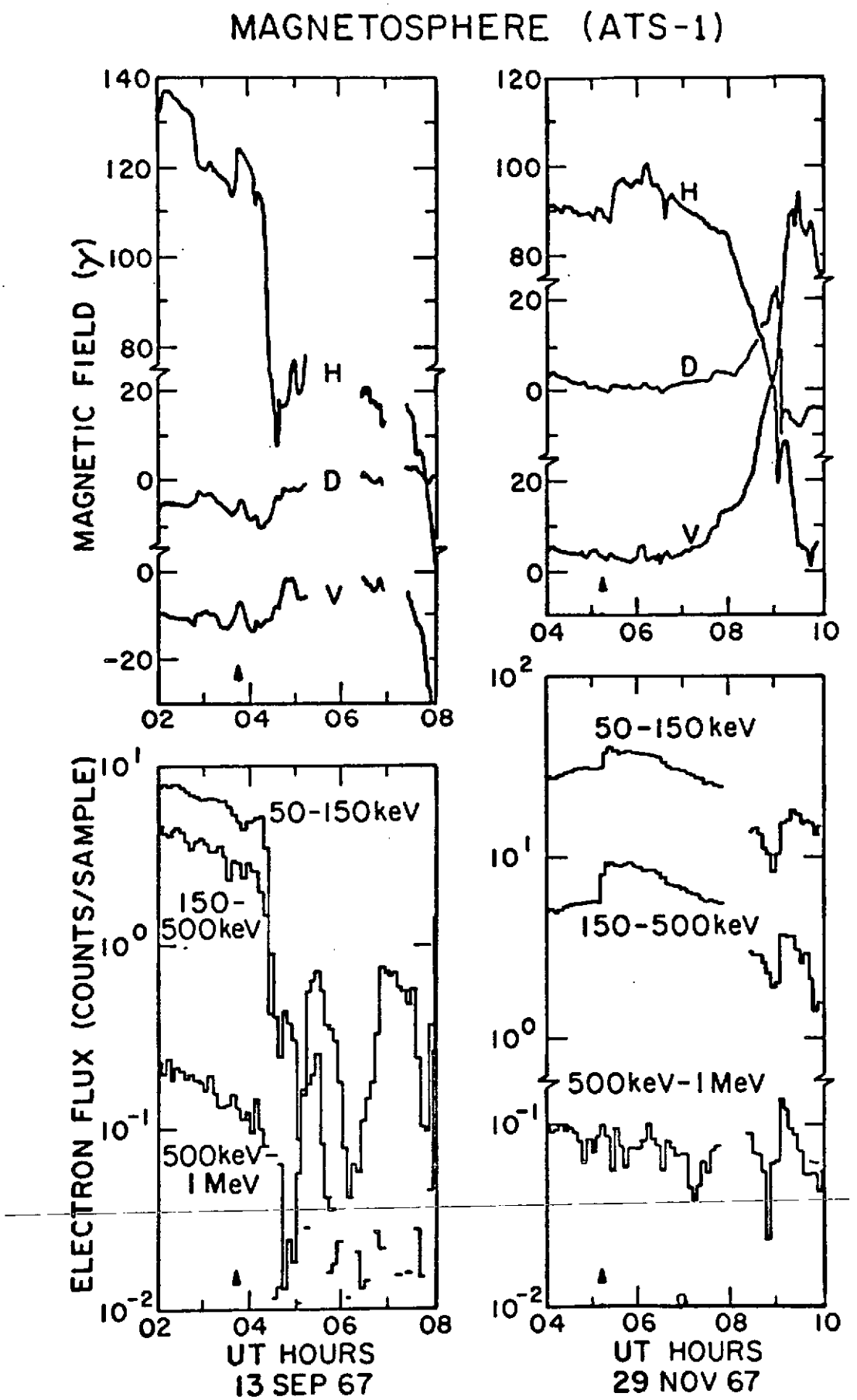
MAGNETOSPHERE (ATS-1)
MAGNETIC FIELD (γ)
H
D
V
ELECTRON FLUX (COUNTS/SAMPLE)
50-150keV
150-500keV
500keV-1MeV
UT HOURS
13 SEP 67
UT HOURS
29 NOV 67

FIGURE 4

HIGH LATITUDE MAGNETIC FIELD

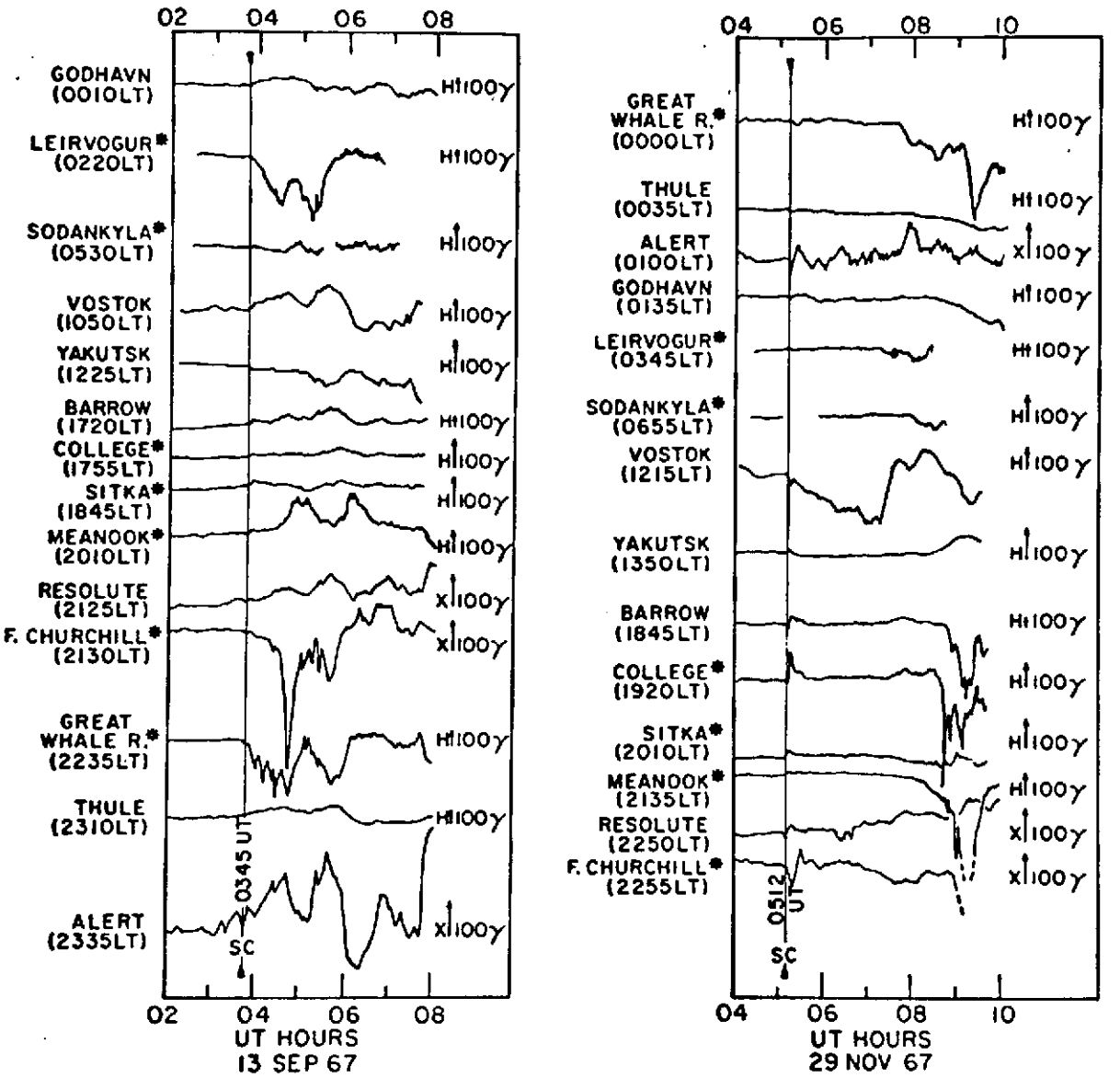

FIGURE 5

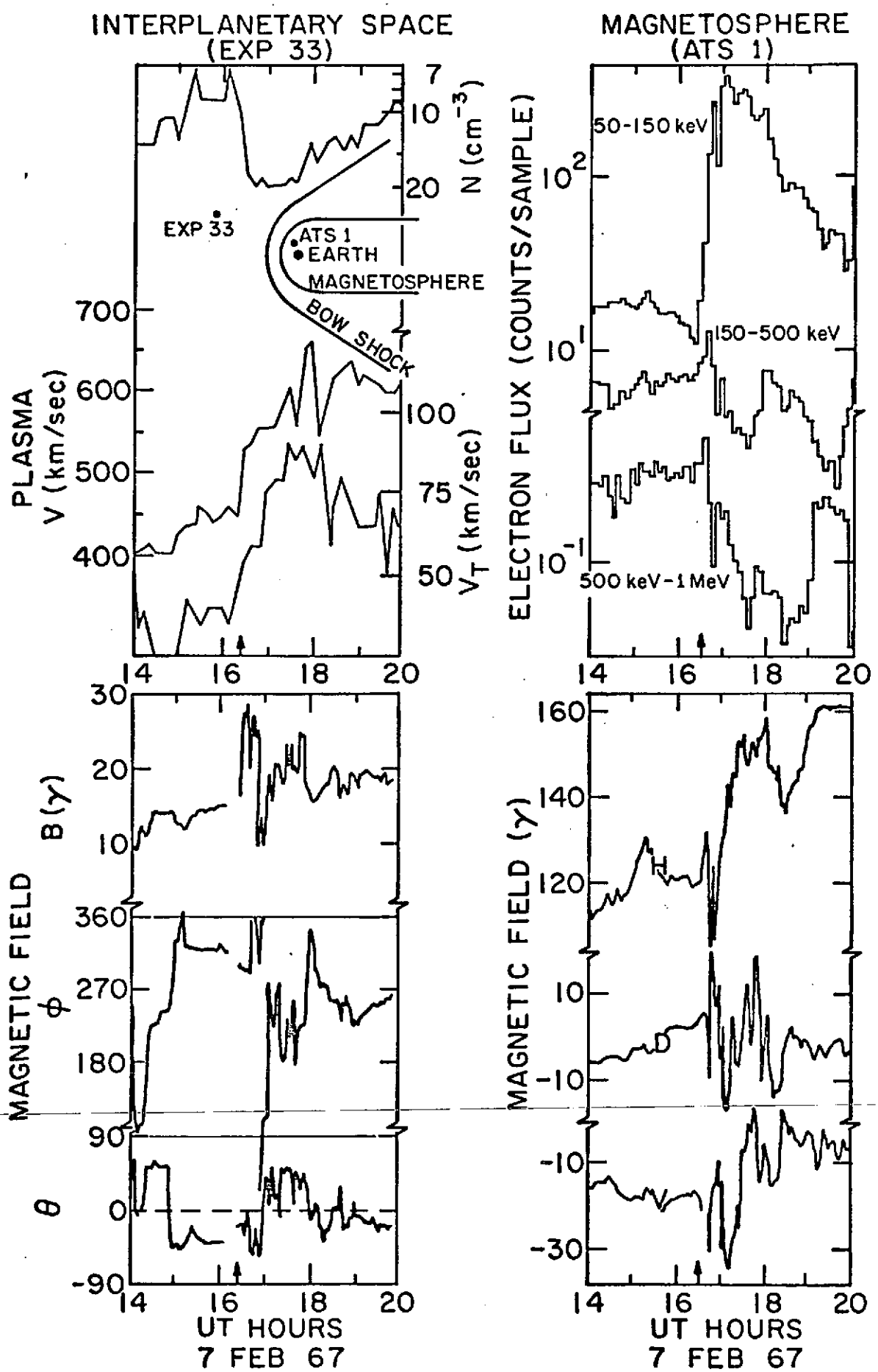
INTERPLANETARY SPACE
(EXP 33)
MAGNETOSPHERE
(ATS 1)
EXP 33
ATS 1
EARTH
MAGNETOSPHERE
BOW SHOCK
PLASMA
V (km/sec)
N (cm⁻³)
V_T (km/sec)
ELECTRON FLUX (COUNTS/SAMPLE)
50-150 keV
150-500 keV
500 keV-1 MeV
MAGNETIC FIELD
B(γ)
φ
θ
MAGNETIC FIELD (γ)
H
D
UT HOURS
7 FEB 67

FIGURE 6

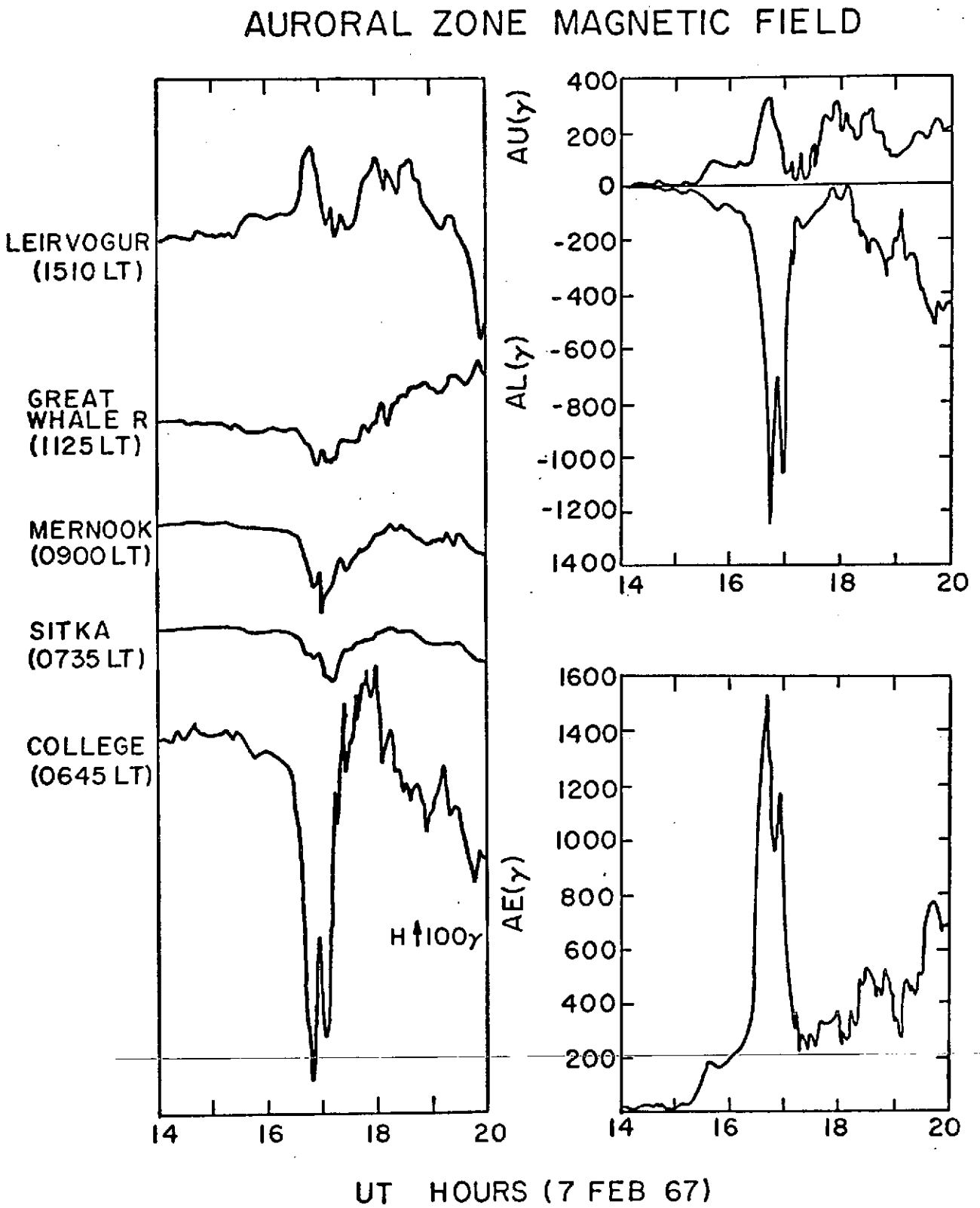
AURORAL ZONE MAGNETIC FIELD
LEIRVOGUR
(1510 LT)
GREAT
WHALE R
(1125 LT)
MERNOOK
(0900 LT)
SITKA
(0735 LT)
COLLEGE
(0645 LT)
H 100γ
AU(γ)
AL(γ)
AE(γ)
400
200
0
-200
-400
-600
-800
-1000
-1200
1400
1600
1400
1200
1000
800
600
400
200
14
16
18
20
UT HOURS (7 FEB 67)

FIGURE 7

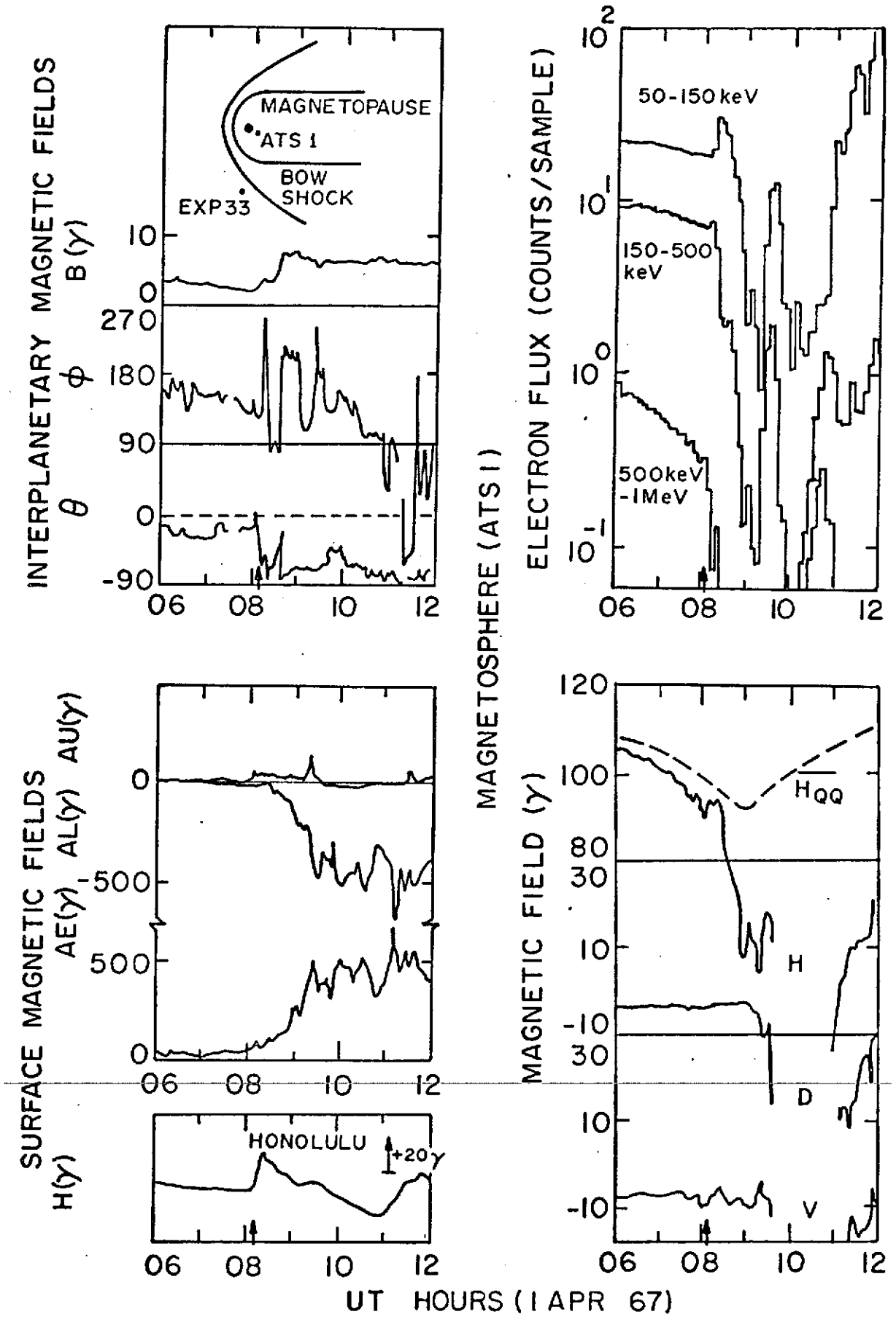
INTERPLANETARY MAGNETIC FIELDS
B(γ)
φ
θ
MAGNETOPAUSE
ATS 1
BOW SHOCK
EXP33
10
0
270
180
90
0
-90
06
08
10
12
MAGNETOSPHERE (ATS 1)
ELECTRON FLUX (COUNTS/SAMPLE)
50-150 keV
150-500 keV
500keV -1MeV
SURFACE MAGNETIC FIELDS
AE(γ), AL(γ) AU(γ)
0
-500
500
H(γ)
HONOLULU
+20γ
MAGNETIC FIELD (γ)
120
100
80
30
10
-10
H
D
V
H_QQ
UT HOURS (1 APR 67)

FIGURE 8

GEOGRAPHIC LOCATION & UNIVERSAL TIME
OF LOCAL MIDNIGHT OF MAGNETOMETER STATIONS

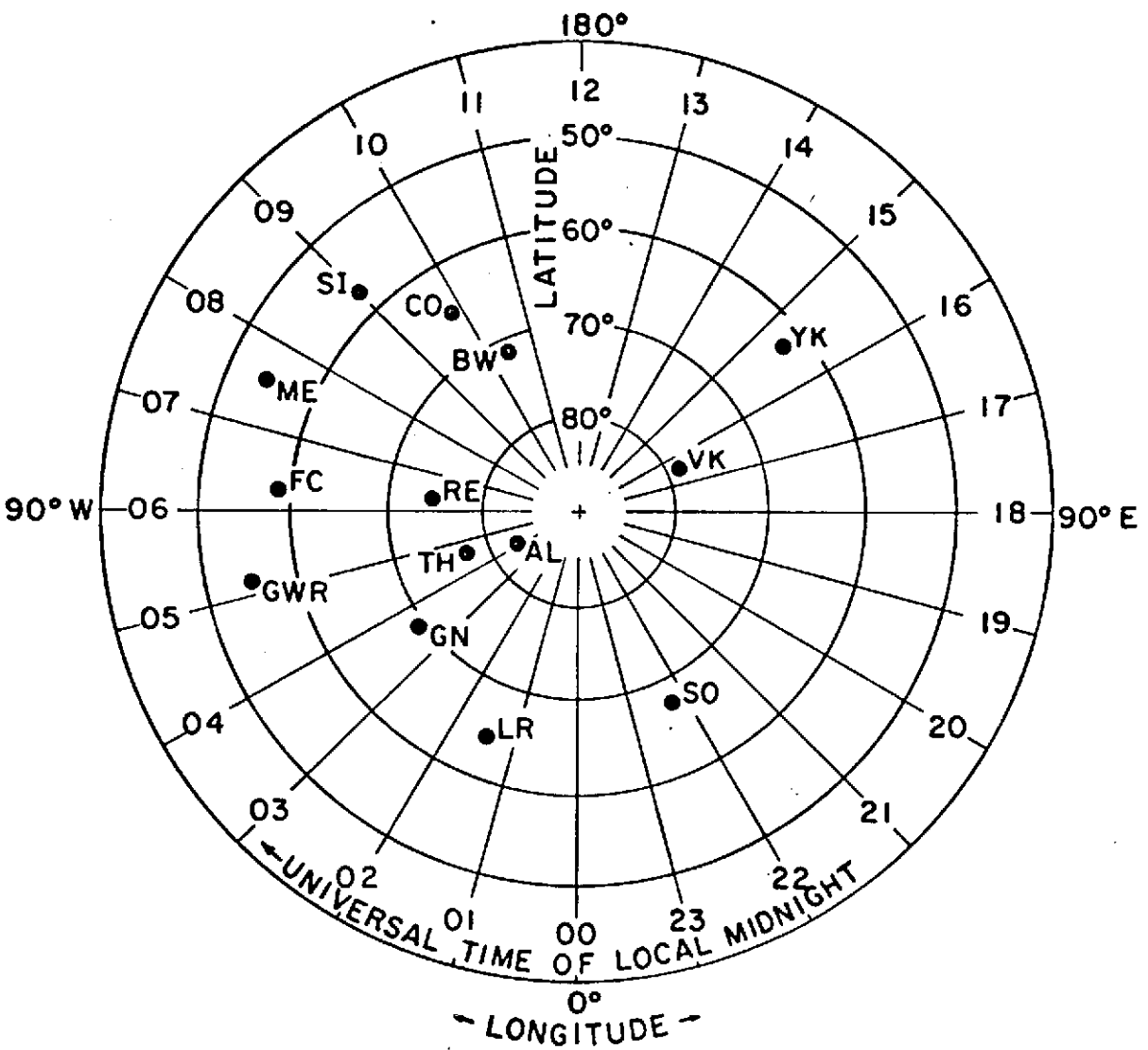

FIGURE 9

GEOGRAPHIC LOCATION & UNIVERSAL TIME
OF LOCAL MIDNIGHT OF A_E STATIONS

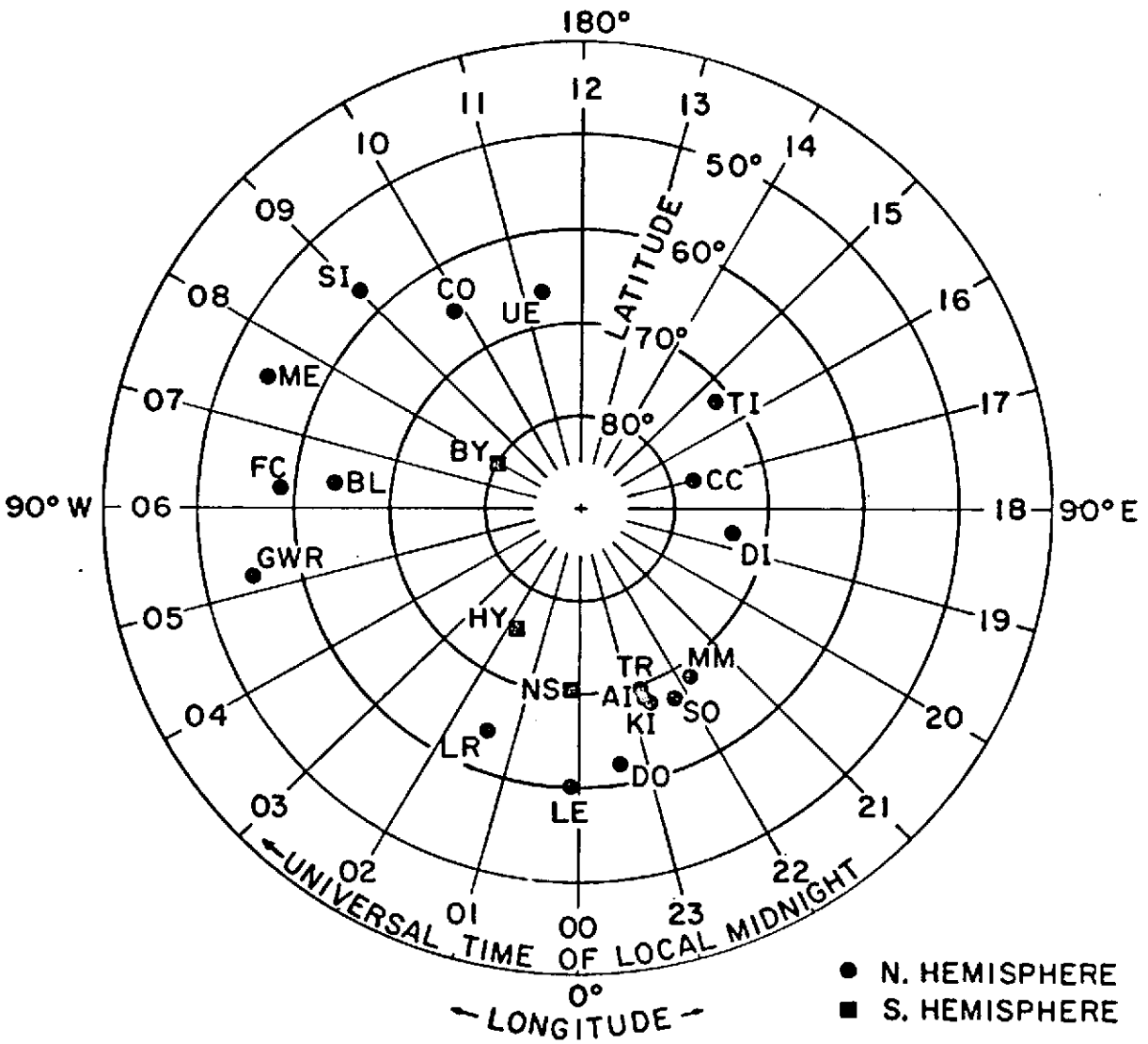

FIGURE 10

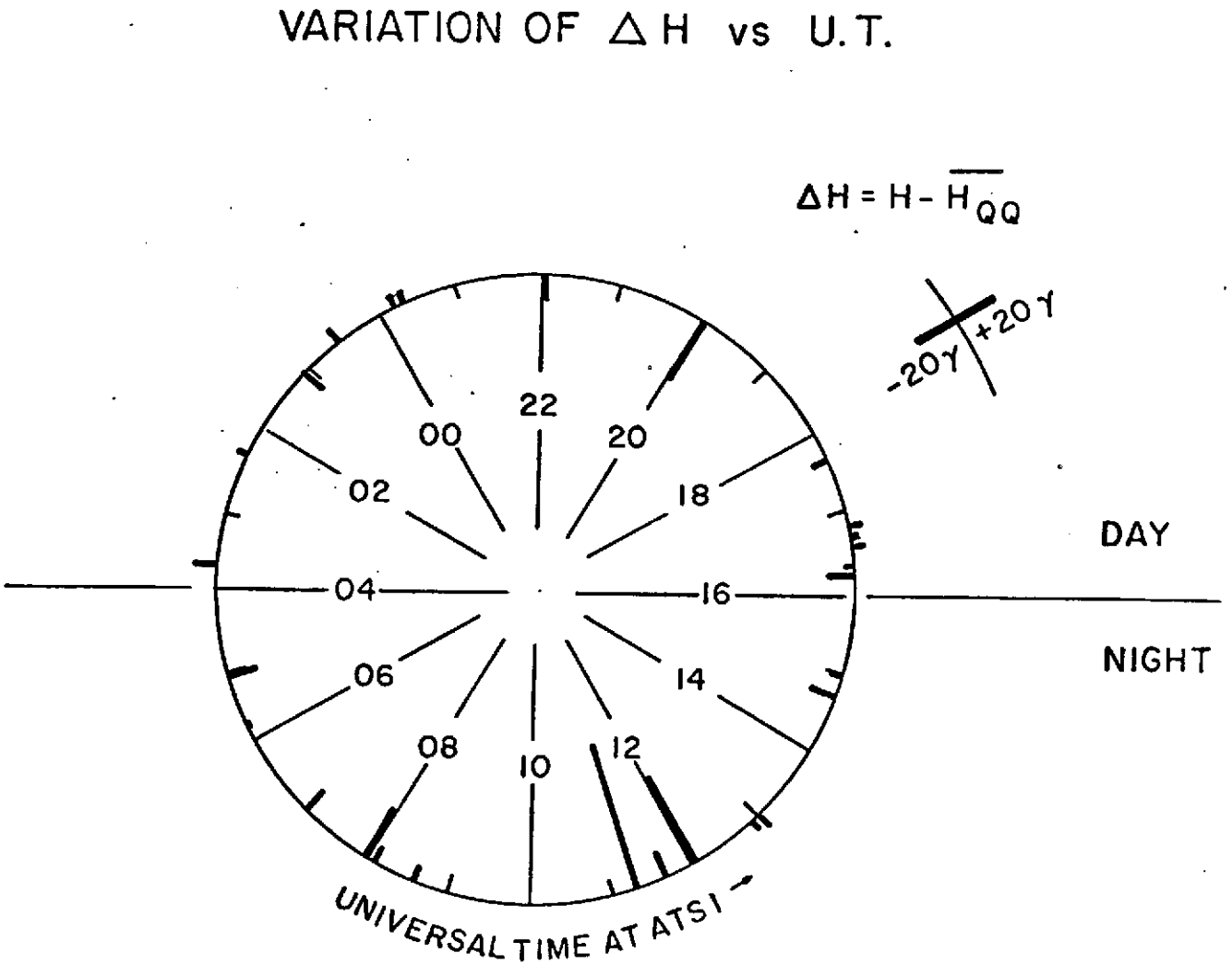
VARIATION OF Δ H vs U.T.
ΔH = H - $\overline{H_{QQ}}$
-20γ
+20γ
22
00
20
02
18
DAY
04
16
NIGHT
06
14
08
10
12
UNIVERSAL TIME AT ATS1

Table 1. Data Available

Event	Date	Sc Time	Sfc. (Mag. Field)		Magnetosphere (ATS 1)		Solar Wind	
			High-lat.	Low-lat.	Mag. Field	El. Flux	Mag. Field	Plasma
1	1-7-67	0759	Yes	Yes	Yes	Yes>50 keV	Yes	No
2	1-13	1200						No
3	2-7	1636						Yes
4	2-15	2347						
5	2-16	0835						
6	4-1	0807						No
7	4-4	0304			No	No		
8	4-23	1426						
9	5-1	1906						
10	5-7	0105			Yes			
11	5-24	1726			No			
12	5-25	1235						
13	6-5	1914						
14	6-25	0221			Yes	Yes	No	Yes
15	6-26	1458			Yes	Yes	No	
16	8-11	0554			No	No	Yes	
17	8-29	1738			Yes	Yes		
18	9-13	0345						
19	9-19	1959						
20	10-28	1637						
21	11-3	1627			No			
22	11-29	0512			Yes			
23	12-18	0538						
24	1-11-68	1251						
25	1-26	1441						
26	2-10	1621						
27	2-14	1253						
28	2-20	1703						
29	2-20	1117						No
30	3-9	2340						Yes
31	5-7	0030				Yes>400 keV		Yes
32	6-10	2154						No
33	6-25	1617						Yes
34	7-3	0812						Yes
35	7-9	2155			No	No		No
36	7-13	1612			Yes	Yes		No
37	7-25	1135			Yes	Yes		No

Table 2. High-latitude Magnetometer Stations and Station Codes

Abisco, Sweden*	AI
Alert, Canada	AL
Baker Lake, Canada*	BL
Barrow, Alaska	BW
Byrd, Antarctica*	BY
Cape Chelyuskin, USSR*	CC
College, Alaska*	CO
Dixon Island, USSR*	DI
Dombas, Norway*	DO
Fort Churchill, Canada*	FC
Godhavn, Greenland	GN
Great Whale River, Canada*	GWR
Halley Bay, Antarctica*	HY
Kiruna, Sweden*	KI
Leirvogur, Iceland*	LR
Lerwick, Great Britain*	LE
Meanook, Canada*	ME
Murmansk, USSR*	MM
Norway Station, Antarctica*	NS
Resolute, Canada	RE
Sitka, Alaska*	SI
Sodankyla, Finland*	SO
Thule, Greenland	TH

Tixie Bay, USSR*	TI
Tromso, Norway*	TR
Uelen, USSR*	UE
Vostok, USSR	VK
Yakutsk, USSR	YK

* Stations used to derive A_E index

Table 3. Data Tabulation for YES-YES Category of Sc Events
(Pre-sc auroral-zone activity with an sc-simultaneous intensification)

		SURFACE	MAGNETOSPHERE		
Sc Date	Sc Time	δH_{SFC}	δH_{ATS}	ΔH_{ATS}	Remarks
1-7-67	0759	+9γ	+8γ	-23γ	Negligible 0759 J disturbance; H depression resumes 0815
1-13	1202	+26γ	+30γ	-40γ	1135 H, J recovery onset
5-7	0105	+10γ	+18γ	-11γ	0125 H depression onset
5-25	1235	+48γ	———	———	———
6-5	1914	+41γ	———	———	———
9-19	1959	+16γ	+18γ	-31γ	Slight J increase 1959; high-energy J depression onset 2030
1-26-68	1441	+23γ	+12γ	-11γ	1500 H depression onset
2-20	0703	+11γ	+3γ	-11γ	0710 H depression onset
6-10	2154	+17γ	+25γ	-13γ	Nothing significant
Average		+22.3γ	+16.3γ	-20.0γ	

Table 3. (cont.)

INTERPLANETARY SPACE

Sc Date	$\overline{B}$	$\overline{\theta}$	$\overline{\phi}$	$\overline{B_Z}$	δB	$\delta\theta$	$\delta\phi$	δB_Z	EXP #	$\overline{V}$	$\overline{N}$	δV	δN	EXP #
1-7-67	12γ	+5°	105°	+1.0γ	12γ→16γ	0°→0°	110°→110°	0γ	28	—	—	—	—	—
1-13	8γ	-20°	295°	-2.5γ	10γ→23γ	-45°→+15°	250°→305°	+13.0γ	33	—	—	—	—	—
5-7	8γ	+25°	215°	+3.5γ	8γ→11γ	+50°→+25°	245°→270°	-1.5γ	33	—	—	—	—	—
5-25	∿11γ	∿0°	∿065°	0	12γ→22γ	0°→0°	90°→90°	0γ	33	—	—	—	—	—
6-5	9γ	-75°	130°	-8.5γ	9γ→21γ	-85°→-85°	180°→285°	-12.0γ	33	—	—	—	—	—
9-19	15γ	-35°	∿280°	-8.5γ	15γ→25γ	-35°→-25°	280°→260°	-2.0γ	33	500 km/sec	3.5/cm³	+90 km/sec	+3/cm³	34
1-26-68	5γ	-30°	085°	-2.5γ	5γ→12γ	-50°→-50°	060°→060°	-5.0γ	33	500 km/sec	0.3/cm³	—	—	34
2-20	2γ	-50°	170°	-1.5γ	—	—	—	—	33	650 km/sec	1/cm³	—	—	33
6-10	—	—	—	—	—	—	—	—	—	—	—	—	—	—
Average	8.8γ	-22°	168°	-2.4γ	10.1γ→18.6γ	-24°→-17°	174°→197°	-1.1γ		550 km/sec	1.6/cm³	—	—	

Table 4. Data Tabulation for NO-YES Category of Sc Events
(No pre-sc auroral-zone activity, but an sc-simultaneous activity onset)

		SURFACE	MAGNETOSPHERE		
Sc Date	Sc Time	$\overline{\delta H}_{SFC}$	δH_{ATS}	ΔH_{ATS}	Remarks
4-1-67	0807	+22γ	+2γ	-6γ	0807 high-energy J depression onset; 0820 H, J_{50-150} depression onsets
4-23	1426	+3γ	—	—	—
5-1	1906	+26γ	—	—	—
5-24	1726	+20γ	—	—	—
6-26	1458	+26γ	+20γ	-3γ	1458: J increases or remains steady
8-11	0554	+30γ	—	—	—
9-13	0345	+9γ	+12γ	+8γ	Negligible 0345 J disturbance; extreme H, J depression onset 0415
1-11-68	1251	+15γ	+4γ	+3γ	1310 H depression onset
2-10	1621	+24γ	+21γ	-3γ	1700 H depression onset
6-25	1617	+12γ	+8γ	+6γ	Nothing significant
7-13	1612	+37γ	+22γ	-6γ	Nothing significant
Average		+20.4γ	+12.7γ	0	

Table 4. (cont.)

INTERPLANETARY SPACE

Sc Date	$\bar{B}$	$\bar{\theta}$	$\bar{\phi}$	$\bar{B}_Z$	δB	$\delta\theta$	$\delta\phi$	δB_Z	EXP #	$\bar{V}$	$\bar{N}$	δV	δN	EXP #
4-1-67	3γ	-20°	135°	-1.0γ	2γ→4γ	-15°→-60°	135°→120°	-3.0γ	33	—	—	—	—	—
4-23	12γ	+25°	130°	+5.0γ	11γ→11γ	+25°→-65°	135°→270°	-14.5γ	33	—	—	—	—	—
5-1	5γ	0°	135°	0	5γ→11γ	+30°→+65°	160°→210°	+7.5γ	33	—	—	—	—	—
5-24	4γ	+40°	140°	+2.5γ	4γ→8γ	+65°→-40°	045°→255°	-8.5γ	33	—	—	—	—	—
6-26	-	—	—	—	—	—	—	—	—	∿400 km/sec	∿0.5/cm^3	+50 km/sec	0	34
8-11	7γ	+10°	∿270°	+1.0γ	5γ→10γ	-25°→-20°	235°→265°	-1.5γ	35	∿430 km/sec	∿6/cm^3	+100 km/sec	+12/cm^3	35
9-13	11γ	-35°	335°	-6.5γ	10γ→15γ	-40°→-40°	335°→315°	-3.0γ	33	370 km/sec	0.3/cm^3	+150 km/sec	0	34
1-11-68	4γ	-15°	290°	-1.0γ	2γ→10γ	-35°→-40°	185°→230°	-5.5γ	33/35	∿425 km/sec	∿0.3/cm^3	+130 km/sec	0	34
2-10	4γ	-25°	325°	-1.5γ	4γ→13γ	-60°→-30°	310°→260°	-3.0γ	33	∿375 km/sec	∿4/cm^3	(+115 km/sec)	(+6/cm^3)	33
6-25	3γ	0°	190°	0	3γ→7γ	-10°→-20°	200°→220°	-2.0γ	33/35	300 km/sec	4/cm^3	(+50 km/sec)	(+5/cm^3)	35
7-13	5γ	∿0°	∿330°	0	8γ→15γ	0°→-35°	315°→315°	-8.5γ	35	—	—	—	—	—
Average	5.8γ	-2.0°	228°	-0.2γ	5.4γ→10.4γ	-6.5°→-28.5°	206°→246°	-4.2γ		383 km/sec	2.5/cm^3	+99 km/sec	(+4/cm^3)	

Table 5. Data Tabulation for NO-NO Category of Sc Events
(No pre-sc auroral-zone activity and no sc-simultaneous activity onset)

		SURFACE	MAGNETOSPHERE		
Sc Date	Sc Time	$\overline{\delta H_{SFC}}$	δH_{ATS}	ΔH_{ATS}	Remarks
4-4-67	0304	+23γ	—	—	—
8-29	1738	+6γ	+5γ	-5γ	1738: J increases or remains steady
11-29	0512	+12γ	+9γ	-15γ	Slight H, J increase 0512
12-18	0538	+28γ	+12γ	-1γ	Slight high-energy J depression onset 0538; H, J_{50-150} depression onset 0600
2-14-68	1253	+6γ	+3γ	+7γ	—
3-9	2340	+11γ	+15γ	+4γ	Nothing significant
5-7	0030	+13γ	+15γ	+6γ	Nothing significant
7-9	2155	+9γ	—	—	—
7-25	1135	+6γ	∿0	-11γ	Nothing significant
Average		+12.7γ	+8.4γ	-2.1γ	

Table 5. (cont.)

INTERPLANETARY SPACE

Sc Date	$\overline{B}$	$\overline{\theta}$	$\overline{\phi}$	$\overline{B_Z}$	δB	$\delta\theta$	$\delta\phi$	δB_Z	EXP #	$\overline{V}$	$\overline{N}$	δV	δN	EXP #
4-4-67	5γ	+15°	115°	+1.5γ	3γ→17γ	-30°→+45°	120°→060°	+13.5γ	33	—	—	—	—	—
8-29	∿5γ	∿+45°	∿330°	+3.5γ	5γ→7γ	+45°→+45°	335°→325°	+1.5γ	33/35	430 km/sec	3/cm³	+30 km/sec	+1/cm³	33
11-29	7γ	+10°	145°	+1.0γ	8γ→15γ	+20°→+30°	160°→160°	+6.0γ	35	390 km/sec	2/cm³	+70 km/sec	fluct.	34
12-18	7γ	∿+50°	285°	+5.5γ	6γ→9γ	+75°→+60°	270°→270°	+2.0γ	33	290 km/sec	0.3/cm³	—	—	34
2-14-68	4γ	+40°	180°	+2.5γ	4γ→5γ	+45°→+45°	180°→180°	+0.5γ	33	370 km/sec	6/cm³	—	—	33
3-9	5γ	+5°	285°	+0.5γ	6γ→10γ	0°→0°	275°→280°	0	35	350 km/sec	4.5/cm³	+30 km/sec	+5/cm³	35
5-7	∿3γ	∿-5°	∿065°	+0.5γ	3γ→6γ	0°→0°	080°→060°	0	35	340 km/sec	8/cm³	+25 km/sec	∿+10/cm³	35
7-9	11γ	+50°	230°	+8.5γ	12γ→15γ	+50°→+55°	230°→230°	+3.5γ	33	—	—	—	—	—
7-25	6γ	+40°	105°	+4.0γ	5γ→8γ	+25°→+65°	120°→045°	+5.5γ	35	—	—	—	—	—
Average	5.9γ	+28°	193°	+2.9γ	5.8γ→10.2γ	+26°→+39°	197°→179°	+3.6γ		362 km/sec	4.0/cm³	+39 km/sec	+5.3/cm³	

Table 6. Data Tabulation for YES-NO Category of Sc Events
(Pre-sc auroral-zone activity, but no sc-simultaneous intensification)

		SURFACE	MAGNETOSPHERE		
Sc Date	Sc Time	$\overline{\delta H_{SFC}}$	δH_{ATS}	ΔH_{ATS}	Remarks
2-15-67	2347	+41γ	+63γ	+5γ	2347 high-energy J depression onset (limited)
6-25	0221	+14γ	+14γ	+2γ	0221: J increases or remains steady
10-28	1637	+21γ	+22γ	+5γ	Nothing significant
11-3	1627	+12γ	___	___	Nothing significant
Average		+22.0γ	+33.0γ	+4.0γ	

Table 7. Data Tabulation for MASKED Category of Sc Events
(Pre-sc auroral-zone activity with an
undetermined sc-simultaneous intensification)

		SURFACE	MAGNETOSPHERE		
Sc Date	Sc Time	δH_{SFC}	δH_{ATS}	ΔH_{ATS}	Remarks
2-7-67	1636	+21γ	-25γ	+3γ	High-energy J depression follows slight 1636 increase
2-16	0835	+34γ	+27γ	-5γ	J recovery underway
2-20-68	1117	+56γ	+50γ	-68γ	1120 H recovery
7-3	0812	+13γ	+5γ	+1γ	~0800 H recovery

Tables 6, 7 (cont.)

INTERPLANETARY SPACE

Sc Date	$\bar{B}$	$\bar{\theta}$	$\bar{\phi}$	$\bar{B}_Z$	δB	$\delta\theta$	$\delta\phi$	δB_Z	EXP #	$\bar{V}$	$\bar{N}$	δV	δN	EXP #
2-15-67	7γ	+45°	255°	+5.0γ	7γ→19γ	+45°→+25°	255°→245°	+3.0γ	33	340 km/sec	12/cm³	+130 km/sec	+14/cm³	33
6-25	—	—	—	—	—	—	—	—	—	∿300 km/sec	∿0.5/cm³	∿+30 km/sec	+0.5/cm³	34
10-28	∿8γ	∿+20°	∿220°	+2.5γ	8γ→14γ	+10°→+20°	230°→220°	+3.5γ	33/35	∿460 km/sec	∿16/cm³	(+40 km/sec)	+3/cm³	35
11-3	∿12γ	∿-40°	∿140°	-7.5γ	12γ→9γ	-45°→-20°	140°→120°	+5.5γ	35	∿460 km/sec	∿3/cm³	(+40 km/sec)	+5/cm³	35
Average	9.0γ	+8°	205°	0γ	9.0γ→14.0γ	+3°→+8°	208°→195°	+4.0γ		390 km/sec	7.9/cm³	+60 km/sec	+5.6/cm³	

Sc Date	$\bar{B}$	$\bar{\theta}$	$\bar{\phi}$	$\bar{B}_Z$	δB	$\delta\theta$	$\delta\phi$	δB_Z	EXP #	$\bar{V}$	$\bar{N}$	δV	δN	EXP #
2-7-67	∿15γ	∿-30°	∿320°	-7.5γ	17γ→28γ	-20°→-20°	300°→300°	-3.5γ	33	500 km/sec	13/cm³	+80 km/sec	+8/cm³	33
2-16	>30γ	+20°	255°	>+10.5γ	16γ→19γ	+40°→-35°	260°→095°	-21.0γ	33	575 km/sec	10/cm³	+25 km/sec	+7/cm³	33
2-20-68	3γ	-5°	360°	-0.5γ	2γ→3γ	-5°→+50°	360°→360°	+2.5γ	33	—	—	—	—	—
7-3	8γ	-45°	305°	-5.5γ	8γ→4γ	-25°→-70°	310°→005°	-0.5γ	35	∿490 km/sec	6/cm³	(-5 km/sec)	(+5/cm³)	35

REFERENCES

Arnoldy, R. L., Signature in the interplanetary medium for substorms, J. Geophys. Res., 76, 5189, 1971.

Aubrey, M. P., and R. L. McPherron, Magnetotail changes in relation to solar wind magnetic field and magnetospheric substorms, J. Geophys. Res., 76, 4381, 1971.

Behannon, K. W., K. H. Schatten, D. H. Fairfield, and N. F. Ness, Trajectories of Explorers 33, 34, and 35: July 1966 - April 1969, Publication No. X-692-70-64, Goddard Space Flight Center, February 1970.

Burch, J. L., Preconditions for the triggering of polar magnetic substorms by storm sudden commencements, J. Geophys. Res., 77, 5629, 1972.

Coleman, P. J., Jr., and W. D. Cummings, Stormtime disturbance field at ATS 1, J. Geophys. Res., 76, 51, 1971.

Coroniti, F. V., Turbulent conductivities in the magnetosphere, Planetary Electrodynamics, Gordon and Breach Science Publishers, New York, 1969, p. 309.

Cummings, W. D., P. J. Coleman, Jr., and G. L. Siscoe, The Quiet-day Magnetic Field at ATS 1, Publication No. 752, Institute of Geophysics and Planetary Physics, University of California, Los Angeles, 1969.

Davis, T. N., and M. Sugiura, Auroral electrojet activity index AE and its universal time variations, J. Geophys. Res., 71, 785, 1966.

De Forest, S. E., and C. E. McIlwain, Plasma clouds in the magnetosphere, J. Geophys. Res., 76, 16, 1971.

Erickson, K. N., and J. R. Winckler, Auroral electrojets and evening sector electron-dropouts at synchronous orbit, J. Geophys. Res., 78, 8373, 1973.

Fairfield, D. H., Polar magnetic disturbances and the interplanetary magnetic field, Space Research VIII, North-Holland Publishing Company, Amsterdam, 1968, p. 107.

Fairfield, D. H., and L. J. Cahill, Jr., Transition region magnetic field and polar magnetic disturbances, J. Geophys. Res., 71, 155, 1966.

Haurwitz, M. W., Auroral substorm activity in relation to storm sudden commencements, ring current effects, and energetic solar protons, J. Geophys. Res., 74, 2348, 1969.

Heppner, J. P., Note on the occurrence of world-wide s.s.c.'s during the onset of negative bays at College, Alaska, J. Geophys. Res., 60, 29, 1955.

Hirshberg, J., and D. S. Colburn, Interplanetary field and geomagnetic variations - a unified view, Planet. Space Sci., 17, 1183, 1969.

Howe, H., J. Binsack, C. G. Wang, and E. Clapp, Explorer 33 and 35 MIT Solar Wind Plasma Data: July 1966 to September 1969, Center for Space Research, Massachusetts Institute of Technology, Cambridge, Massachusetts, 1971.

Kawasaki, K., S.-I. Akasofu, F. Yasuhara, and C.-I. Meng, Storm sudden commencements and polar magnetic substorms, J. Geophys. Res., 76, 6781, 1971.

Kokubun, S., Polar substorm and interplanetary magnetic field, Planet. Space Sci., 19, 697, 1971.

Lezniak, T. W., and J. R. Winckler, Experimental study of magnetospheric motions and the acceleration of energetic electrons during substorms, J. Geophys. Res., 75, 7075, 1970.

Lin, C. S., G. K. Parks, and J. R. Winckler, Particle redistribution conserving first and second adiabatic invariants, to be published (1974).

Meng, C.-I., B. Tsurutani, K. Kawasaki, and S.-I. Akasofu, Cross-correlation analysis of the AE index and the interplanetary magnetic field B_Z component, J. Geophys. Res., 78, 617, 1973.

Ness, N. F., K. W. Behannon, S. C. Cantarano, and C. S. Scearce, Early results from the magnetic field experiment on lunar Explorer 35, J. Geophys. Res., 72, 5769, 1967.

Parks, G. K., G. Laval, and R. Pellat, Behavior of outer radiation zone and a new model of magnetospheric substorm, Planet. Space Sci., 20, 1391, 1972.

Perona, B. E., Theory on the precipitation of magnetospheric electrons at the time of a sudden commencement, J. Geophys. Res., 77, 101, 1972.

Roederer, J. G., The earth's magnetosphere, Science, 183, 37, 1974.

Roederer, J. G., and E. W. Hones, Jr., Motion of magnetospheric particle clouds in a time-dependent electric field model, J. Geophys. Res., 79, 1432, 1974.

Rostoker, G., and C.-G. Fälthammar, Relationship between changes in the interplanetary magnetic field and variations in the magnetic field at the earth's surface, J. Geophys. Res., 72, 5853, 1967.

Russell, C. T., The configuration of the magnetosphere, Critical Problems of Magnetospheric Physics, National Academy of Sciences, November 1972, p. 1.

Schatten, K. H., and J. M. Wilcox, Response of the geomagnetic activity index Kp to the interplanetary magnetic field, J. Geophys. Res., 72, 5185, 1967.

Schieldge, J. P., and G. L. Siscoe, A correlation of the occurrence of simultaneous sudden magnetospheric compressions and geomagnetic bay onsets with selected geophysical indices, J. Atm. Terrest. Physics, 32, 1819, 1970.

Swift, D. W., A mechanism for energizing electrons in the magnetosphere, J. Geophys. Res., 70, 3061, 1965.

Tsurutani, B. T., and C.-I. Meng, Interplanetary magnetic-field variations and substorm activity, J. Geophys. Res., 77, 2964, 1972.

Van Allen, J. A., On the electric field in the earth's distant magnetotail, J. Geophys. Res., 75, 29, 1970.

Wilcox, J. M., K. H. Schatten, and N. F. Ness, Influence of interplanetary magnetic field and plasma on geomagnetic activity during quiet-sun conditions, J. Geophys. Res., 72, 19, 1967.